

Advances of Smart Stimulus-Responsive Microneedles in Cancer Treatment

Huaqing Chu, Jiangtao Xue, Yuan Yang, Hui Zheng,* Dan Luo,* and Zhou Li*

Microneedles (MNs) have emerged as a highly promising technology for delivering drugs via the skin. They provide several benefits, including high drug bioavailability, non-invasiveness, painlessness, and high safety. Traditional strategies for intravenous delivery of anti-tumor drugs have risks of systemic toxicity and easy development of drug resistance, while MN technology facilitates precise delivery and on-demand release of drugs in local tissues. In addition, by further combining with stimulus-responsive materials, the construction of smart stimulus-responsive MNs can be achieved, which can respond to specific physical/chemical stimuli from the internal or external environment, thereby further improving the accuracy of tumor treatment and reducing toxicity to surrounding tissues/cells. This review systematically summarizes the classification, materials, and reaction mechanisms of stimulus-responsive MNs, outlines the benefits and challenges of various types of MNs, and details their application and latest progress in cancer treatment. Finally, the development prospects of smart MNs in tumor treatment are also discussed, bringing inspiration for future precision treatment of tumors.

with the advancement of innovative chemotherapeutic, targeted, immunotherapeutic, and genetic drugs, as well as the quest for functional preservation and aesthetics in patients with cancer, radical surgery has now been gradually replaced by drug treatment combined with small-scale minimally invasive surgery.^[2] Nevertheless, to date, eradication of tumor cells has remained a challenge, which results in poor control or even recurrence of the cancer. Traditional drug administration routes, including oral administration, intravenous injection, intramuscular injection, mucosal administration, transdermal administration, etc., have their own challenges.^[3,4] For example, oral administration involves the first-pass hepatic biotransformation^[5]; intravenous administration, as a systemic-acting mode of drug delivery, causes greater damage to normal tissues/cells^[6,7];

intramuscular injection faces problems of painful injections, fear of needles, and high demands on injection techniques^[8,9]; mucosal delivery needs to improve the stability of the dosage form^[10]; traditional transdermal patch have difficulty in breaking through the physical barrier formed by the stratum corneum (SC)^[11,12] the above problems potentially impede the clinical treatment of tumors. To enhance the effectiveness and safety of anti-tumor therapy, it is crucial to create a novel delivery approach that can efficiently and specifically transport antitumor agents (such as chemotherapeutic drugs, immunosuppressants, immune cells, tumor vaccines, photosensitizers (PSs), photothermal agents, etc.) to the intended tissues. This will enable precise and personalized treatment, while also improving patient compliance and comfort.

The emergence of microneedles (MNs) is a result of significant progress in materials science and micro-nanofabrication technologies. MNs typically comprise an assortment of micro-sized needles with consistent characteristics affixed to a supporting base on one side, enabling superior mechanical penetration.^[13,14] These MNs can enter the SC and create temporary microchannels on the skin to achieve effective drug administration, so as to exert local or even systemic therapeutic effects.^[15,16] Based on its outstanding advantages of painlessness, non-invasiveness, convenience, high patient compliance, relative safety, and high drug bioavailability,^[17,18] the MNs technology has emerged as a highly potential transdermal drug delivery system (TDDS) that effectively combines the benefits of conventional transdermal patch

1. Introduction

Cancer is a significant global public health issue that poses a severe threat to human life and well-being.^[1] In recent decades,

H. Chu, H. Zheng
Department of Anesthesiology
National Cancer Center/National Clinical Research Center for Cancer/Cancer Hospital
Chinese Academy of Medical Sciences and Peking Union Medical College
Beijing 100021, China
E-mail: zhenghui@cicams.ac.cn

H. Chu, J. Xue, D. Luo, Z. Li
Beijing Institute of Nanoenergy and Nanosystems
Chinese Academy of Sciences
Beijing 101400, China
E-mail: luodan@binn.cas.cn; zli@binn.cas.cn

J. Xue
School of Medical Technology
Beijing Institute of Technology
Beijing 100081, China

Y. Yang
Institute of Process Engineering
Chinese Academy of Sciences
Beijing 100190, China

 The ORCID identification number(s) for the author(s) of this article can be found under <https://doi.org/10.1002/smt.202301455>

DOI: 10.1002/smt.202301455

and subcutaneous injection.^[19] Over the past several decades, MNs have been fabricated using various constituent materials, from silicon,^[20] metals,^[21] ceramic,^[22,23] and glass^[24,25] to polymers^[26] and hydrogels.^[27] Traditional MNs face challenges in accurately delivering the required medication dosage to the desired location at the optimal moment to maintain a stable level of the drug in the bloodstream, and excessive drug load can easily lead to drug resistance and safety issues.^[28]

Benefiting from the development of responsive biomaterials and manufacturing technology,^[29] stimulus-responsive MN-based therapy system arises at a historic moment, making on-demand drug delivery feasible.^[30] Researchers often refer to MNs with the characteristics of personalized drug delivery such as adaptability, controllability, surrounding environmental perception, and real-time feedback as “smart MNs”.^[31–33] This individualized, demand-based drug delivery process (also known as “on/off”), with excellent spatial-, temporal- and dosage-controlled properties.^[34,35] The stimulus-responsive MNs therapeutic system can programmatically release drugs based on pathological characteristics or exogenous physical/chemical signals to achieve the purpose of cancer treatment.^[36–40] In this review, the classification, materials, fabrication process, response mechanism, advantages, and disadvantages of stimulus-responsive MNs were systematically discussed. Subsequently, the application and latest progress of stimulus-responsive MNs in cancer treatment are introduced in detail. Finally, current research hotspots, future prospects, and challenges of stimulus-responsive MNs are meticulously discussed.

2. Classifications of Stimulus-Responsive MNs

In recent decades, there has been a widespread use of responsive nanomaterials in the development of intelligent pharmaceutical delivery systems.^[41,42] The combination of stimulus-responsive materials and MNs delivery technology has become a popular research area in recent years for the development of controlled release systems based on MNs. Stimulus-responsive MNs can specifically recognize special signals from endogenous or exogenous environments and generate accurate responses. The stimulation factors can elicit several changes in MNs, including deterioration of the matrix, swelling of the matrix, rupture of the formulation, and collapse of the coating.^[43] The MNs-based delivery system, which responds to stimulus, allows for precise regulation of medication release, leading to a significant enhancement in therapeutic effectiveness and a reduction in harmful side effects.^[28] Stimulus-responsive MNs can be classified into two categories based on the source of the stimulus signals: endogenous stimulus-responsive MNs and exogenous stimulus-responsive MNs (Figure 1).

2.1. Exogenous Stimulus-Responsive MNs

Recently, there has been a growing interest in exogenous stimulus-responsive MNs due to their capacity to achieve medication release that can be controlled remotely, resulting in improved therapeutic efficacy and lower toxicity to the body. According to actual clinical needs, such MNs can precisely control

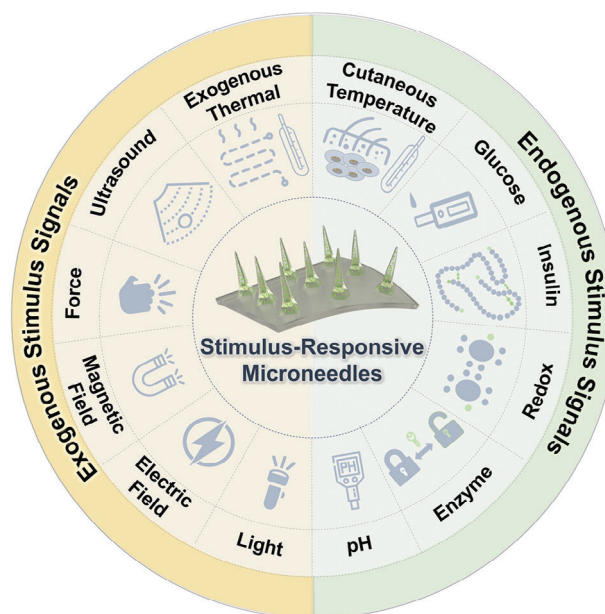


Figure 1. Schematic of classification of stimulus-responsive microneedles. According to different types of stimulation signals, stimulus-responsive microneedles are divided into exogenous and endogenous microneedles. Endogenous stimulation signals include changes in pH, glucose, insulin, enzyme, redox, cutaneous temperature, etc., while exogenous stimulation signals include changes in ultrasound, light, electric field, force, magnetic field, and temperature.

the immediate and on-demand release of drugs through external stimulation signals (such as ultrasound, light, electricity, force, magnetic field, temperature change, etc.), which is a more controllable and safe delivery mode. In Table 1, we summarize a series of recent research on exogenous stimulus-responsive MNs for biomedical treatment.

2.1.1. Ultrasound-Responsive MNs

Ultrasound is a type of mechanical wave that has a frequency higher than 20 kHz and is able to travel through a certain media.^[44] Ultrasound has been employed as an effective non-invasive stimulus in drug delivery systems.^[45] In terms of mechanism, the cavitation effect and thermal effect of ultrasound can achieve spatiotemporally targeted drug release.^[46,47] A small portion of the ultrasound energy is absorbed by the tissues of the human body, causing localized heating that promotes drug release. As shown in Figure 2A, the utilization of ultrasound induces the generation, oscillation, expansion, and subsequent rupture of microbubbles (MBs), commonly referred to as the cavitation effect. This mechanism is often employed to elucidate the principle of drug release in response to ultrasound. Studies have shown that the extracorporeal ultrasound-assisted MNs patch has significantly improved the efficiency of transdermal drug delivery.^[48–50] Most typically, Zandi et al.^[48] reported an ultrasound-assisted MNs drug delivery system named zinc-oxide nanowires microbubble generator probe (ZnONWs-MGP). Excessive MBs were exploded by external ultrasonic actuation (an intensity of 5 W cm⁻², a frequency of 20 kHz, and a duty cycle of 30%), and subsequently induced microcavitation in tumor

Table 1. Summary of exogenous stimulus-responsive MNs.

Stimuli	Responsive compositions	Applications	Drugs	Animal Models	References
Ultrasound	Microbubbles generated by MNs, Nanobubbles on the MNs surface, HA	Anti-tumor treatment Controlled Drug-Delivery	Paclitaxel Cy5 Rhodamine B	breast cancer model	[48] [49, 50]
Light	Photothermal agents (Fe ₃ O ₄ NPs, ICG, LaB ₆ , AuNPs, Au Nanocage, Au Nanoshell, Au Nanorod, BP, GO, Cu ₂ S ₄ , CuS, MOF, NIR950 micelles, Bi nanodots, polydopamine, melanin tumor lysate, PPy hollow fibers, MXene)	Cancer therapy epilepsy treatment PTT and Chemotherapy PTT, Immunotherapy PTT, Chemotherapy, targeted therapy Wound Care Diabetic wound healing	phenobarbital 5-Fu, doxorubicin, docetaxel, Camptothecin, doxorubicin granulocyte-macrophage colony-stimulating factor, indoleamine 2,3-dioxygenase Thrombin, temozolomide, bevacizumab NO, Hb, adenosine Metformin, insulin lidocaine hydrochloride IFN- γ , Dexamethasone ibuprofen doxorubicin neutral red, safranine T L-DOPA Dexamethasone, EGF	PNG-induced epilepsy mice A431 and A375 tumor-bearing mice, Melanoma mice model, 4T1 breast tumors triple-negative breast cancer 4T1 carcinoma tumor mice Human xenograft: Glioblastoma model wound infection mice cutaneous wound type I diabetes rat model STZ-induced diabetic rats SLE animal model xenograft mouse melanoma model, subcutaneous 4T1 tumor-bearing mouse model mouse acne model	[53] [57–59, 62, 65, 68–70, 72, 76, 85] [63, 79] [61] [64, 74] [73, 78, 80] [66, 71, 81, 82] [60] [67] [55] [55, 58, 75] [56, 77] [52] [83]
Electric current	Azo, β -CD-modified poly(acrylic acid) Azo, upconversion micron-rods PPy, poly(ethyleneimine), 1-vinylimidazole, Au, Ag, MXene, salmon deoxyribonucleic acid,	Controlled drug release Parkinson's disease treatment treating psoriasis-like skin disease, AD, Neuroinflammation,	Indomethacin, lidocaine, L-ascorbic acid Rhodamine B insulin insulin crystal violet, insulin, Minoxidil	Imq-induced psoriasis-like model mice, DNCB-induced AD-bearing mouse model, Spinal cord injuries rats rabbit incisor pain model injury model of the swine skin diabetic rats STZ-induced T1D mice	[36, 87–89] [90, 91] [93, 99] [94] [98] [104, 105]
Mechanical force	Alginate microgel, polymethyl methacrylate	Antipyretic analgesic effects Controlled drug release Blood Coagulation Diabetes therapy Diabetes therapy			
Magnetic field	atomized iron powder, RdFeB particles, mesoporous iron oxide nanoraspberry	Controlled drug release, Diabetes therapy, Androgenetic alopecia treatment		Diabetic minipig models, hair growth experiment model mice	[107–109]
Exogenous temperature	Tridecanoic acid, SCMC, Dodecanoic acid-cetylamine salt, PCL	Diabetes monitoring and therapy Pain management against emergent ionizing radiation injury	metformin Cy5 G-CSF	STZ-induced diabetic rats, Genetically derived diabetic animal model	[112–115]

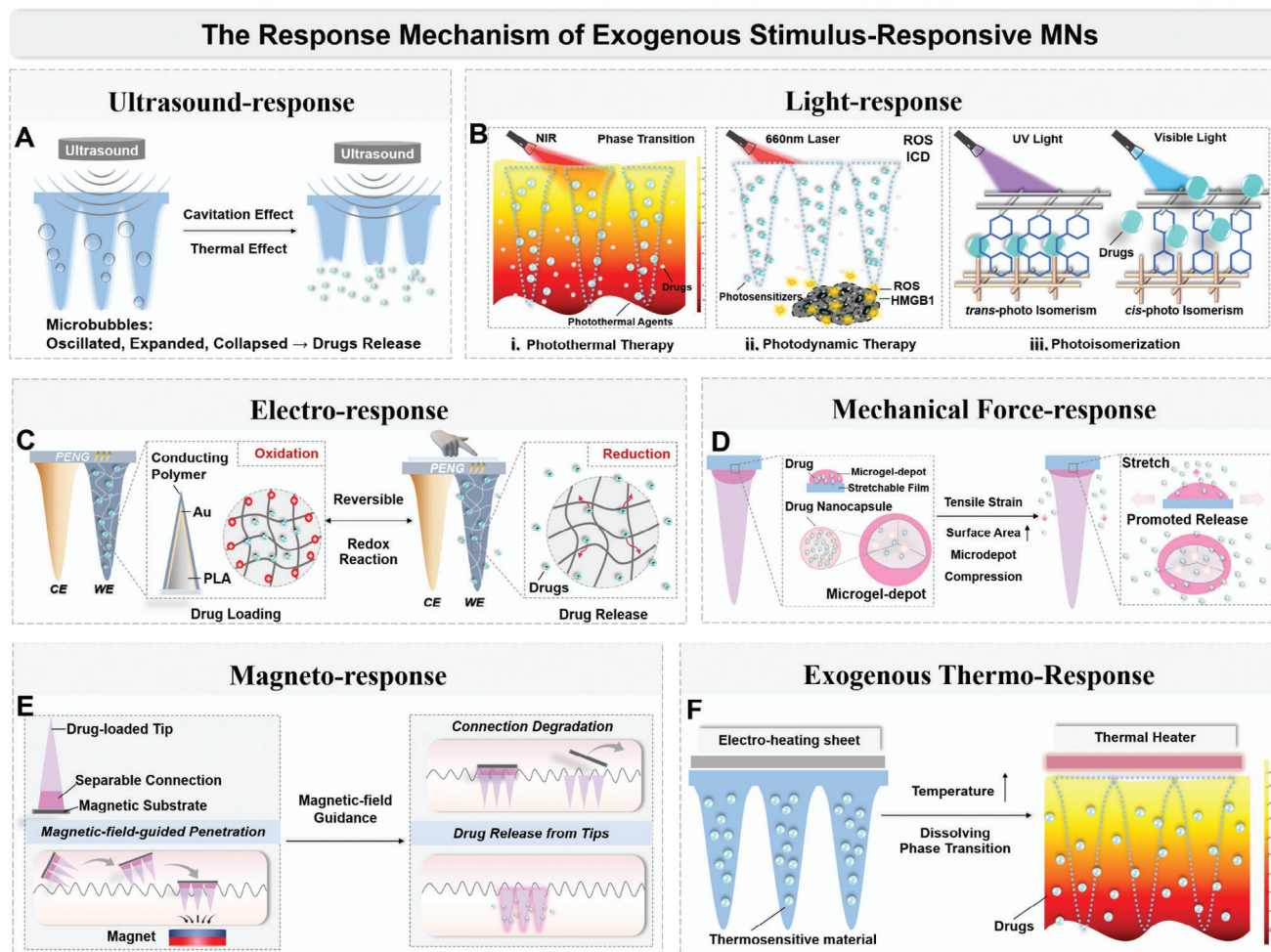


Figure 2. Schematic of the responding mechanism of different exogenous stimulus-responsive microneedles. A) Spatiotemporally targeted drug release can be realized based on the cavitation effect and thermal effect of ultrasound waves. Microbubbles formed, oscillated, expanded, collapsed, and finally triggered drug release when ultrasound was applied. Reproduced with permission.^[50] Copyright 2020, Springer Nature. B) Drug release mechanisms based on light-responsive microneedles. i) Under light irradiation, the temperature of photothermal-based microneedles increases and undergoes phase transition, which promotes drug release. Reproduced with permission.^[57] Copyright 2016, American Chemical Society. ii) Photodynamic-based microneedles trigger photosensitizers (PS) to undergo REDOX reactions by light irradiation and produce a large number of reactive oxygen species (ROS), which promote local cell rupture and necrosis. In addition, PDT can trigger immunogenic cell death, which activates an anti-tumor immune response. Reproduced with permission.^[54] Copyright 2021, American Chemical Society. iii) Under light irradiation, the material molecules of photoisomerization-based microneedles undergo reversible changes in *cis*-conformation and *trans*-conformation, which can realize light-controlled drug release. Reproduced with permission.^[52] Copyright 2017, The Royal Society of Chemistry. C) Electro-responsive MNs prepared by conductive polymers control drug on-demand release through the “on-off” of electrical signals. Upon electrical stimulation (ES), the REDOX state of the conductive polymer will be reversibly changed, resulting in drugs loaded and controlled release. Reproduced with permission.^[87] Copyright 2021, WILEY. D) Daily body movement or intentional stretching can cause strain of the elastomer in the mechanical force-responsive microneedles, increase the surface area for diffusion and Poisson’s ratio-induced compression on the microdepots, thus promoting the release of drugs from the microdepots. Reproduced with permission.^[104] Copyright 2015, American Chemical Society. E) A magneto-responsive separable MN robot was constructed via a Lego-brick-stacking-inspired multistage 3D fabrication method. The MN robot consists of three components: the magnetic substrate, the separable connection, and the drug-loaded tips. Under the guidance and control of the external magnetic field, the magnetic substrate faces the small intestinal wall, penetrates the intestinal mucosa, breaks the intestinal barrier, and continuously releases the encapsulated active substances. Reproduced with permission.^[108] Copyright 2021, WILEY. F) An external heater is integrated with thermo-responsive MNs prepared from a thermosensitive phase change material (PCM). When the embedded microheater is heated above a threshold temperature, the MNs dissolve and release the packaged drug. Reproduced with permission.^[115] Copyright 2018, Informa UK.

cells, promoting the direct transfer of paclitaxel (PTX) into cancer cells. Shao et al.^[49] developed a patch of MNs that has been modified with nanobubbles. This patch is intended for medication delivery with the assistance of ultrasound (a frequency of 850 kHz, an amplitude of 10 V_{pp}, a power of 1 W cm⁻²). The MNs patch was made of poly(D,L-Ladppctic-Co-Glycolic Acid)

(PLGA), a good biocompatible and degradable material. The surface of the MNs patch was coated with polylysine (PLL) to create a layer of positive charge. This layer then attracted and bonded with a layer of fluorescent dye-containing nanobubbles that carried a negative charge, through electrostatic contact. Layer-by-layer (LBL) self-assembled Cy5-containing nanobubbles adhered to the

surface of the MNs underwent oscillation, expansion, and collapse, and subsequently initiated the release of Cy5 with the application of ultrasound. Cavitation-induced microstreaming increased drug molecule penetration and diffusion, hence enhancing the effectiveness of transdermal drug administration. The *ex vivo* data demonstrated that a mere 2 min of ultrasound stimulation led to a fivefold increase in the amount of released material, as compared to passive release during a 10 min period. The benefit of this particular design is that by immediately loading micro/nanobubbles onto the MNs, the diffusion efficiency is enhanced, while simultaneously reducing the required ultrasound energy and preventing any harm to the body caused by ultrasound. More interestingly, the optimal integration of ultrasonic responsiveness and iontophoresis effectively enhanced the efficacy of transdermal medication administration. Bok et al.^[50] developed multifunctional hyaluronic acid (HA)-dissolving MNs, in which the vibration caused by acoustic pressure and the electrostatic force-driven diffusion caused by AC iontophoresis synergistically promoted the dissolution of the HA MNs and drug release. By subjecting gelatin hydrogels to MNs, the bubbles within the hydrogel are compressed, resulting in the formation of microjets due to the sound pressure generated by ultrasonic waves at a frequency of 1.7 MHz. This process greatly enhances the efficiency of drug delivery (Figure 2A). In conclusion, the combined use of ultrasonic waves with iontophoresis offers a notable benefit by enhancing the rate at which drugs are delivered via the skin using MNs. This approach facilitates the penetration and dispersion of drug molecules.

Although ultrasound-responsive MNs can control the drug release process non-invasively and accurately. Nevertheless, ultrasonic waves have a dose-dependent effect on the damage to healthy tissue. To minimize the negative impact of ultrasound-responsive MNs on healthy tissue during their use, it is crucial to meticulously choose and optimize ultrasound parameters. In addition, part of the energy of the ultrasound may be absorbed in the tissue, which will make its effect in the deep tissue greatly reduced. The cooperation of ultrasound equipment increases the complexity and cost of treatment.

2.1.2. Light-Responsive MNs

Light is considered to be an attractive trigger for constructing on-demand TDDS due to its advantages of remoteness, precise control of temporal and spatial dose, and ease of application.^[39,40] Photo-responsive MNs are prepared by specific photosensitive materials that respond specific wavelength of light (e.g., ultraviolet (UV) light,^[51] visible light,^[52–56] near-infrared (NIR) light,^[57–83] etc.). UV light has the ability to destroy biological molecules (nucleic acid, protein, and lipid), and has high absorption and scattering in tissues, which limits its clinical application. Visible light is mainly used for the superficial layer of skin and mucous membranes. NIR is widely concerned because of its advantages of low scattering, strong penetrability, and little tissue damage.^[84] Regarding methodologies for photosensitive material response, photo-controlled drug delivery platforms can be broadly categorized into three types: photothermal, photochemical, and photoisomerization-based drug delivery (Figure 2B).

Photothermal-Based MNs: The MNs system based on photothermal therapy (PTT) consists of two key components: 1) photothermal agents that effectively transform the energy of light into thermal energy; 2) heat-sensitive materials that somehow respond quickly to temperature changes and lead to drug release (Figure 2B(i)). So far, photothermal agents that are commonly used include oxide (Fe_3O_4 nanoparticles (NPs)),^[60,64] indocyanine green (ICG),^[63,68,72] lanthanum hexaboride (LaB_6),^[57–59] gold nanomaterials (gold nanocage,^[65] gold NPs,^[53] gold nanoshell,^[61] gold nanorod^[69,70]), black phosphorus,^[66,67,80] carbon nanomaterials (graphene and its derivatives),^[78] metal sulfides (Cu_7S_4 ,^[82] CuS ^[62]), MXene,^[73] aggregation-induced emission luminogen (AIEgen),^[76] melanin tumor lysate,^[79] metal–organic frameworks (MOFs),^[74] Polypyrrole (PPy) hollow fibers,^[85] and so on. These photothermal agents possess a high capacity for absorbing light, exhibit remarkable efficiency in converting light into heat, and demonstrate outstanding stability. When a specific wavelength of light was irradiated externally, the MNs occurred light-to-heat transformation, and the temperature of the surrounding tissue increased in a short time, resulting in local thermal ablation and direct killing of the pathological cells. Simultaneously, when the temperature rose, the thermally responsive material of MNs experienced a phase shift, facilitating the release of pharmaceuticals and serving the dual purpose of drug therapy and photothermal treatment (Figure 2B(i)). PTT has been widely used in biomedicine because it can be controlled remotely and has fewer side effects than traditional treatments, especially in tumor treatment. For instance, Dong et al.^[65] designed a dissolving MNs loaded with gold nanocage and doxorubicin (DOX). Gold nanocage was a drug nanocarrier used for controlled drug release, to enhance the mechanical properties of MNs, and to exert PTT for skin tumors. After the MNs were applied to the skin, the bodies of the MNs were dissolved and DOX was released. The gold nanocage acted as a photothermal agent under NIR light, prompting a significant increase in local temperature and enhancing the damage to the tumor cells. The anti-tumor efficacy of the DOX- and gold nanocages-loaded MNs was demonstrated by a melanoma mice model. At the same time, pathological imaging was used to observe the vital internal organs of mice after MNs administration. The results showed that there were no obvious abnormal changes in the histology of the animal organs, indicating that the delivery system had good biocompatibility.

In addition, despite photothermal-based MNs having many advantages, there are still some problems. The temperature change caused by photothermal action may cause discomfort, damage to the body, and inactivation of effective biomolecular activity. Therefore, the illumination time and photothermal transition temperature must be controlled accurately and reasonably in practical applications.

Photochemical-Based MNs: The mechanisms by which photochemical-based MNs exert therapeutic benefits are as follows: 1) The objective is to disrupt the photosensitive covalent connections within the MNs platform by absorbing light energy, which triggers the release of the enclosed medication. Light of adequate energy is necessary for the cleavage of photolabile covalent bonds. For instance, the ester bond might undergo irreversible cleavage when exposed to UV radiation. Hardy et al.^[51] employed UV radiation to cleave the covalent ester link of ibupro-

fen conjugates, resulting in the production of the unbound drug and 2-phenyl-5, 7-dimethoxybenzofuran; 2) Light irradiation induces the generation of a significant quantity of reactive oxygen species (ROS), which in turn triggers PSs to undergo REDOX reactions. This process promotes local cell rupture and necrosis, resulting in the cytotoxicity observed in photodynamic treatment (PDT). In addition, PDT has the ability to induce immunogenic cell death, thereby stimulating the body's immune system to respond against the tumor (Figure 2B(ii)).^[54–56,75] To address the limitations of PDT in tumor treatment (ineffective local migration of PSs and rapid oxygen consumption), Liu et al.^[56] developed an oxygen-propelled MNs patch loaded with chlorin e6 (Ce6) and embedded sodium percarbonate (SPC). After the MNs were applied to the tissue, SPC reacted with the surrounding fluid to produce gaseous oxygen bubbles, which promoted the penetration of Ce6 with a strong airflow flow. Through the delivery of oxygen-propelled Ce6 and the improvement of the hypoxic environment, the intracellular ROS in the tumor tissue was greatly increased, and the PDT effect in the intradermal breast cancer mouse model was enhanced.

However, the photochemical-based MNs have some drawbacks. First of all, the process of drug release caused by photocissible covalent bond breakage is usually irreversible, which means these delivery systems are often “one-and-done”, making it impossible to generate uniform “on-off” release curves from each light exposure as other pulsatile drug release systems. Second, the breakage of covalent bonds in this system mostly requires to be driven by UV light, but UV light will destroy biological molecules (such as DNA and growth factors) and has poor penetration, so it is only suitable for superficial applications. Although PDT has many advantages, as a local therapy, its killing effect on tumors largely depends on whether the light dose in the diseased area is sufficient. However, some PSs can cause biological damage under high concentrations or excessive irradiation. The treatment efficacy of PDT is somewhat constrained by the reduction in light intensity resulting from tissue absorption and dispersion.^{fl}

Photoisomerization-Based MNs: The delivery of drugs through photoisomerization can be accomplished by causing reversible changes in the molecular structure under UV–vis light exposure. Azobenzene (azo) is a commonly chosen compound for drug delivery systems that rely on photoisomerization. The molecules consist of two phenyl groups linked by an N=N bond, which undergo a transition from trans conformation to cis conformation when exposed to UV light, then revert back to trans conformation when exposed to blue light.^[86] In recent years, researchers have taken advantage of this reaction characteristic to create the molecular valve, which can realize the “turn on/turn off” drug release by remote light control (Figure 2B(iii)).^[52,83] To prevent harm from UV radiation, upconversion luminescent materials were used. These materials can convert biocompatible NIR light into local UV–vis light. This conversion process is used to trigger the cis-trans isomerization of azo.^[83]

It's worth noting that photoresponsive MNs may generate new photosensitive groups and degradation products during the triggering process, some of which are toxic. Hence, there is a pressing need to discover and cultivate advanced photosensitive materials that possess superior biosecurity and can disintegrate and dispense medications at reduced temperatures.

2.1.3. Electro-Responsive MNs

The electro-responsive MNs are superior to other externally triggered MNs because of their excellent repeatability, ease of acquisition, ease of manipulation, and low intensity without causing noticeable discomfort to the human body. The fundamental concept behind the electro-responsive drug delivery system using MNs is to encapsulate pharmaceuticals within a carrier composed of MNs and utilize an electric field to enhance or regulate the release of the drugs. The research of these smart MNs is around the design and fabrication of electro-responsive MNs, as well as the advancement of energy supply systems. Currently, commonly used electrical responsive materials include conductive polymers,^[87–89] conductive hydrogels,^[90–92] carbon-based materials, some metals,^[93] semiconductor materials,^[94] etc.

Conductive polymers, such as PPy, Polyaniline, Polythiophene, and its variants, are characterized by high conductivity, easy production, and good biocompatibility. Drug delivery systems based on biomaterials derived from MNs have been extensively utilized for the regulated release of several medications, including dexamethasone, epidermal growth factor, dopamine, and others. Upon electrical stimulation (ES), the REDOX state of the conductive polymer will be reversibly changed, resulting in changes in charge, doping level, conductivity, and volume of the conductive polymer. Taking advantage of this property, drug-loaded MNs prepared by conductive polymers control drug on-demand release through the “on-off” of electrical signals (Figure 2C). In the case of PPy, when a negative voltage is given to PPy, the oxidized PPy undergoes reduction, resulting in a decrease in the overall positive charge on the molecular chain. This weakens the electrostatic attraction and causes the anionic medicines to be repelled and freed from the polymer system. Applying a positive voltage to PPy causes an oxidation reaction, resulting in a rise in the positive charge of the molecular chain. This leads to the release of the cationic medication due to electrostatic repulsion. The release of neutral medicines is primarily propelled by polymer deformation. Huang et al.^[89] developed an innovative transdermal medication delivery system consisting of an electro-responsive PPy-coated MN array. They fabricated conical MNs using microscale 3D photolithography and then sputter-coated the MNs with chrome-gold. Then, the electrochemical deposition of PPy film on the surface of chromium-gold coated MN electrodes was completed by the galvanostatic method, and dexamethasone phosphate was encapsulated in the PPy coating to form the working electrode. The drug-loaded MNs were inserted epidurally, penetrating the dura, in order to administer pharmaceuticals directly to the subdural area, thus providing localized drug administration. Experiments have shown that the release of dexamethasone phosphate from cyclic voltammetry-stimulated PPy MNs via the dura mater can potentially play a therapeutic role. Similarly, based on this property of PPy, Yuan et al.^[88] developed a two-electrode smart MNs patch consisting of a polylactic acid-platinum (PLA-Pt) array as the counter electrode and a polylactic acid-platinum-polypyrrole (PLA-Pt-PPy) material. The MN array functioned as the working electrode.

Conductive hydrogels possess the advantageous characteristics of both conductive materials and hydrogels, including excellent conductivity, stability, and mechanical qualities. Conductive hydrogels exhibit high sensitivity, and electrostimulation induces

changes in various properties of hydrogels, including phase, volume, shape, optics, mechanics, surface area, reaction rate, and recognition performance.^[95,96] The gadget, known as the electro-modulated hydrogel-MNs, was created using conductive hydrogels that were loaded with drugs.^[97] Upon penetrating the skin, MNs absorbed the fluid found between cells in the skin and expanded, resulting in a certain level of conductivity. Subsequently, medication release was regulated by applying electrical stimulation. For example, Indermun et al.^[90] developed a transdermal system called electro-modulated hydrogel-MNs array (EMH-MNA) that includes a ceramic MN array with nano-sized pores and an optimized EMH. This system is designed to administer indomethacin in a controlled manner by responding to electrical stimulation. The medication was typically covered in a hydrogel under normal conditions. The medication was released into the skin upon activation with an electro-stimulus. When the electro-stimulus was turned off, the drugs stopped being released. Another method used to produce controlled drug release by electrostimulation in accordance with the iontophoresis concept involved the integration of conductive hydrogels with porous or hollow MNs as the drug reservoir. In order to penetrate the mouth mucosa and underlying bone tissue with drugs, Seeni et al.^[91] created a unique conductive MNs array that was combined with the iontophoresis approach. Through the utilization of this platform, the researchers achieved a twofold enhancement in the conductivity of MNs and a 30% reduction in the electrical resistance of mouse skin. These improvements had a substantial impact on the concentration of drugs administered to the skin, resulting in a large rise. Additionally, certain investigations have employed the iontophoresis process to regulate medication release.^[50,98]

Metal materials such as gold, silver, and magnesium have high thermal and electrical conductivity, biocompatibility, and easy processing, which have been widely favored in conductive drug-loaded MNs. In general, the application of voltage to metal or metal-coated MNs can induce electrochemical reactions and electrothermal conversion effects to regulate the rate of drug delivery. The back of each polyvinylpyrrolidone (PVP)-MNP was coated with gold or silver by Yang et al.^[93] utilizing the thermal evaporation technique to maximize drug release efficiency and provide superior thermal and electrical conductivity. In particular, the experimental result showed that the drug release efficiency increased more than 7.9 or 5.3 times when electric voltage or ~40°C heat was applied. Furthermore, a semiconductor is a substance that exhibits a conductivity level between that of a conductor and an insulator at normal room temperature, and its conductivity may be manipulated. MXenes are a type of innovative 2D structural material that consists of transition-metal carbides, nitrides or carbonitrides. They possess the properties of graphene, such as high specific surface area and conductivity. Additionally, MXenes offer the advantages of flexibility, adjustable components, and the ability to control the minimum nanolayer thickness. A multifunctional MNs system based on MXenes nanosheet was created by Yang et al.^[94] It is a “hospital-on-a-chip” with real-time biosensing, electrostimulation, and medication release capabilities. Researchers integrated an electrostimulator with drug-loaded MNs to expedite the clotting time of bleeding by employing specific frequency voltage pulses generated by the electrostimulator.

At present, the commonly used power supply methods of electroresponsive MNs drug delivery systems include traditional commercial power sources,^[88] wireless communication circuits,^[98] self-driven nanogenerators (piezoelectric nanogenerator (PENG), triboelectric nanogenerator (TENG)).^[87,92,99] The next generation of wearable healthcare systems is primarily focused on the development of wireless technology and self-power technology, which offer a more flexible and manageable structure compared to traditional batteries.^[100] For the real-time monitoring and management of diabetes, Li et al.^[98] developed an integrated wearable closed-loop system (IWCS) based on Bluetooth wireless technology for mobile devices. The IWCS comprised three modules: 1) Utilizing mesoporous magnetic NPs for the purpose of reversing iontophoretic extraction and electrochemical sensing; 2) Developing a flexible printed circuit board (FPCB) that is integrated and controlled; 3) Creating a component for iontophoretic insulin delivery using MNs. The entire device can be worn on the human arm. Upon penetration of the MNs through the outermost layer of the skin (SC), the glucose present in the fluid surrounding the cells was drawn into the sensor chamber using a process called reverse iontophoresis. Subsequently, an electrochemical detection method was employed using a three-electrode system. The flexible circuit module examined the captured glucose signals and transmitted them to an external smartphone via Bluetooth wireless communication. The FPCB transmitted control signals and activated the MNs drug delivery device, which administered insulin using iontophoresis when hyperglycemia was detected. This smart system can realize real-time monitoring, intelligent response, trackable data, and quantitative management; however, the wireless signal transmission required complex circuit design, which led to the structure design difficulty, process difficulty, and cost of the entire device increased dramatically, greatly affecting the popularization and application of this system. Researchers have recently combined nanogenerators with drug-loaded MNs to create a self-powered programmable TDDS. This system regulates drug release by harnessing biomechanical energy (such as motion, bending of joints, breathing, and heartbeat) and converting it into electrical energy.^[87,99] As shown in Figure 2C, this self-powered MNs system utilizes biomechanical energy as its only energy source, eliminating the need for external devices. This advancement enhances the convenience of drug delivery systems and offers a viable wearable technique for on-demand drug delivery in the treatment of diverse disorders. A more comprehensive investigation yielded the development of a self-powered transcutaneous electrical stimulation system in Minnesota. This system was created by integrating a sliding free-standing triboelectric nanogenerator (sf-TENG) with two-stage MN patches.^[36] The sf-TENG transformed the mechanical energy produced by finger sliding into a biocompatible microcurrent and conducted ES using conductive MNs. The self-powered ES can function as an “adjuvant” to suppress the glutathione (GSH)-mediated decrease of epiderma growth factor (EGF) by controlling the molecular movement, guaranteeing the stability of EGF. Both laboratory experiments (in vitro) and experiments conducted on living organisms (in vivo) showed that the ES increased the expression of epiderma growth factor receptor (EGFR) and enhanced the process of receptor desensitization. This system also enhanced the effectiveness of EGF in promoting wound healing through

many mechanisms. Collectively, this work revealed that the ES of electroresponsive MNs is no longer limited to promoting drug release, but will also improve drug pharmacodynamics from the level of drug action mechanism, creating a new therapeutic strategy for electrostimulation therapy.

Although electro-responsive MNs have numerous advantages, they face numerous challenges. For example, how to improve the precise manufacturing technology of electro-responsive MNs, how to stably exist the prepared drug-carrying conductive polymers, the biological safety of electro-responsive MNs in the treatment process (whether there is short-term or long-term damage to nerve pathways, cells, tissues, etc. by external electrical stimulation), and the production cost and feasibility in practical application scenarios must all be addressed one by one.

2.1.4. Mechanical Force-Responsive MNs

Mechanical force, which can be categorized as compressive, tensile, and shear pressures, is present throughout the body and in various daily activities. Examples include muscle tension, organ and tendon tension, bone and joint tension, as well as compression in cartilage and bones.^[101] Convenient commands enable the therapy of various ailments by easily accessing mechanical stimuli.^[102] In biomedical applications, pressure-responsive hydrogels have shown significant advances.^[103] These hydrogels are particularly flexible, highly sensitive, and repeatable, which allows their use in both single and cyclic pressure feedbacks. Hydrogel systems with these unique properties typically respond to external stress in their characteristics. A mechanical force-triggered MN system can be built to release drugs when simple movements of body parts or external forces are applied as stimulus signals. As is shown in Figure 2D, Di et al.^[104] created a drug delivery system that is activated by tensile strain. This system consists of a wearable patch with an array of MNs, coupled with a highly stretchy elastomer and cross-linked microgel that contains drug-loaded NPs. Regular physical activity or deliberate stretching can lead to the stretching of the elastomer in the system, which in turn increases the surface area for diffusion and compression on the microdepots due to Poisson's ratio. This ultimately enhances the release of medicines from the microdepots. Based on this therapeutic technique, diabetes can easily control their blood glucose levels (BGLs) by daily body motions. However, since this system released most of the drugs in the first strain cycle, it was difficult to achieve a delivery mode of long-term controlled release. Furthermore, Jiang et al.^[105] created a patch of touch-actuated MNs array for the controlled release of liquid macromolecular medicines. The device comprised a dense array of MNs, a medical adhesive tape, a leak-proof gasket, and a medical sponge. The MNs were firmly incorporated into the liquid drug reservoir, and the medication's passive diffusion was regulated by touch-activated "push and release" operations. Upon pressing the MNs patch with a finger, the MNs, which were in solid form, successfully pierced through the sponge and the SC layer, reaching the skin tissue. This action resulted in the formation of temporary aqueous microchannels on the surface of the skin. When the pressure was removed, the solid MNs detached from the skin, and then the drug was rapidly delivered through the microchannel into the skin tissue for disease treat-

ment. Over time, the microchannel narrowed gradually due to the skin's healing process. The medication administration ceased once the microchannel underwent self-closure. Ultimately, the delivery of the medicine through the patch of MNs arrays allows for precise control of dosage by utilizing the process of reopening and self-closure of microchannels in the skin.

Put simply, the mechanical force-mediated trigger could allow for the quick delivery of medications in a way that patients can give themselves. However, there are still some problems to be solved, such as how to reduce drug residue in the storage layer, how to determine the quantitative relationship between pressure and dosage, and so on. For example, future research on the problem of drug residues in the storage layer can be explored from the following aspects: optimization of the structure of MNs, introduction of auxiliary agents in the storage layer to promote dissolution, adjustment of drug crystal and particle size and other parameters to reduce residue, and recovery of residual drugs to reduce drug waste. In short, it is imperative to do additional research on the internal mechanism of the mechanical force-responsive system in order to enhance the therapeutic efficacy and mitigate the risk of drug overdose in the future.^[102]

2.1.5. Magneto-Responsive MNs

Magnetic induction technology possesses the attributes of long-distance guidance, resilience in complex conditions, adaptability, etc.^[106] It holds significant potential in the fields of surgical guidance, drug delivery, and blood testing. The magnetic responsive materials used in the existing research include atomized iron powder,^[107] NdFeB particles,^[108] mesoporous iron oxide (MIO),^[109] etc. These magnetic materials can be driven wirelessly by a magnetic field.^[110] By means of applying an external magnetic field, it will induce material deformation or directional movement to the specific magnetic direction. Skillfully, Jayaneththi et al.^[107] investigated wireless magnetically responsive MNs for controllable drug release. In this study, the deformation of magnetic polymer composites was induced by an external magnetic field to control drug delivery through single hollow MNs. The gadget, devoid of on-board electronics or batteries, utilized an inductive sensing mechanism to wirelessly detect the reservoir volume, hence allowing for tracking of dose and medication dispensation. Similarly, Fang et al.^[109] created a transdermal composite consisting of magnetically responsive MNs that were filled with minoxidil and encapsulated with MIO nano-raspberry. This composite was developed for the purpose of treating androgenetic alopecia. The application of an external magnetic field triggered an elevation in the local temperature, facilitating the release of the medication. Meanwhile, the cutaneous blood vessels were vasodilated and blood flow increased, which promoted hair regeneration. In view of the various advantages of magneto-responsive microrobots in the biomedical field, Zhang et al.^[108] combined drug-loaded MNs with magnetically responsive microrobots to create a novel oral drug delivery system specifically designed for macromolecular medicines. The research team developed a magnetically sensitive and detachable MN robot using a 3D building approach inspired by stacking Lego bricks. Figure 2E illustrates the composition of these MN robots, which have three main elements: the magnetic substrate,

the detachable connection, and the drug-loaded tips. Guided by the external magnetic field, the magnetic substrate positioned itself against the wall of the small intestine and entered the intestinal mucosa, thereby disrupting the intestinal barrier and releasing the enclosed active chemicals in a continuous manner. The magnetic substrate can be safely evacuated with the help of intestinal peristalsis. This study revealed the immense potential and tangible utility of magneto-responsive MNs in the oral delivery of many medication kinds, including macromolecules and bioactive medicines.

Overall, it is likely that the integration of magnetic induction and MNs technology will expand the use of wearable intelligent systems in the biomedical field and enable the development of advanced smart responsive devices. At the same time, it should be noted that the magneto-responsive MNs need to be equipped with external magnetic field equipment or a magnetic field generator, which reduces the convenience of use. The magnetic response may limit the selection of some special treatment scenarios or magneto-sensitive materials. In addition, the safety of magneto-responsive materials and strong magnetic fields to organisms needs further study.

2.1.6. Exogenous Thermo-Responsive MNs

Thermo-responsive medication administration is a well-researched approach that is particularly focused on wound management and tumor therapy. It has been extensively studied and explored. Thermo-responsive MNs are typically regulated by a non-linear, abrupt alteration in the characteristics of at least one constituent of the nanocarrier substance in response to temperature.^[34] It is important to mention that temperature-responsive hydrogels are the most commonly employed smart hydrogels. The thermos-responsive hydrogels undergo structural or mechanical alterations that are temperature-dependent.^[111] The thermosensitive hydrogel that is most commonly investigated is N-isopropylacrylamide (NIPAM) hydrogel, which has a lower critical solution temperature (LCST). Specifically, such hydrogel has a phase transition process around LCST (33 °C): when the external temperature is lower than 33 °C, NIPAM hydrogel absorbs water and expands, and the hydrogel is colorless and transparent. When the external temperature rises to 33 °C or higher, the hydrogel will shrink suddenly and the phase transition will occur. At this time, the hydrogel will become white turbidity.

One strategy to fabricate thermo-responsive MNs is to integrate an external heater with MNs.^[112–114] Upon reaching a predetermined temperature, the implanted microheater causes the bioabsorbable polymer MNs, which are coated with a phase-change material (PCM), to dissolve and subsequently release the enclosed medicament. Specifically, polycaprolactone (PCL), which has excellent biocompatibility and a relatively low melting temperature, was chosen as the material for the needle in order to facilitate heat-triggered drug release (Figure 2F).^[115] This work involved the creation of distinct MNs that can be easily separated. These MNs were designed for the purpose of delivering metformin via the skin of diabetic rats. Once the detachable MNs arrowheads were completely inserted into the skin, they were subjected to an electric-heating sheet, resulting in the

melting of the PCL MNs at a temperature of ≈ 50 °C. Upon the swift phase change of the PCL from solid to liquid, the encapsulated medicines were discharged. Moreover, Lee et al.^[112] prepared flexible translucent smart MNs by doping gold particles in graphene and combining them with a gold mesh. The integrated MN patch contained a series of sensors that detected humidity, glucose levels, pH, and temperature. Tridecanoic acid acted as a thermally active bioresorbable layer that coated the MNs. Upon detecting elevated glucose levels in sweat, the patch activated the embedded heater, causing the PCM of MNs to melt. This, in turn, facilitated the release of metformin for the treatment of diabetes. In addition, a medication delivery system created by Yin et al.^[113] combined MNs with microheaters that were 3D manufactured. Experimental results showed that the patch could well control the speed of drug release and the depth of penetration by adjusting the temperature of the microheater. Similarly, Yu et al.^[114] created a wearable system for recombinant human granulocyte colony-stimulating factor (G-CSF). To create naked MNs, HA solutions containing G-CSF were cast into the mold. Given that the dodecanoic acid-cetylamine salt (DA-CM) had a significantly lower and more appropriate melting temperature range of 40–41 °C, the solvent hexane did not impact the effectiveness of G-CSF in the MNs. Ultimately, DA-CM was chosen as a temperature-sensitive coating layer in order to produce temperature-responsive MNs. The study involved the production of flexible heaters by the application of jet printing techniques using Ag NP inks. When mice wearing GWS were exposed to a radiation environment and reached the starting dose rate threshold, the γ -ray sensor was quickly activated. The heater worked immediately, and the thermosensitive coating layer of MNs melted rapidly when heating to 45 °C. Immediately, G-CSF was released rapidly, exerting the therapeutic effect in time. Lately, the photothermal converters facilitated the conversion of light into heat, resulting in an increase in the temperature of the target tissue. This rise in temperature caused the temperature-responsive MNs to melt, thereby controlling the release of medicines. For details, see section “2.1.2 Light-Responsive MNs”.

Although some progress has been made in the study of thermo-responsive MNs, there are still some problems. For example, LCST hydrogels only respond to temperature, and their functions are relatively simple. The limited biodegradability of most LCST hydrogels hinders their utilization in the biomedical domain. Long-term exposure of skin to elevated temperature is easy to cause thermal damage.

2.2. Endogenous Stimulus-Responsive MNs

Physiological parameter variations serve as significant indicators for various diseases, including cancer, endocrine disease, degenerative diseases, autoimmune disorders, infectious diseases, and cardiovascular diseases. These variations provide valuable insights for the development of therapeutic systems that respond to endogenous stimuli in the form of MNs.^[29] In contrast to the passive drug delivery method of the exogenous stimulus-responsive MNs system, the endogenous responsive MNs system can autonomously control the release of drugs in response to dynamic changes in biochemical signals. This allows for a personalized treatment process that is both efficient and responsive to

specific needs. This type of MNs does not necessitate the use of any additional apparatus to ensure drug delivery as needed. Furthermore, it exhibits heightened sensitivity, aligning with therapeutic requirements, and possesses considerable research importance and promise. So far, the most studied endogenous biochemical stimuli include pH, glucose, insulin, REDOX reaction products, enzymes, cutaneous temperature, and so on. In Table 2, we summarize a series of recent research on endogenous stimulus-responsive MNs for biomedical treatment.

2.2.1. pH-Responsive MNs

Different organs and tissues have specific pH ranges.^[116] Normal human skin has a somewhat acidic pH, often ranging from 4.2 to 5.6. The epidermis maintains a pH level of ≈ 5.5 , and skin cancer typically develops within this particular layer of the skin.^[117] Meanwhile, pathological circumstances, such as cancer, inflammation, infection, ischemia, and hypoxia, can significantly influence the pH value. This characteristic makes pH an ideal stimulus signal in controlled medication release systems. In inflammatory sites or tumor tissues, it is feasible to control drug release by pathological pH value due to changes in local metabolism and microenvironment. Primarily, this particular type of MNs patch is created by either directly utilizing pH-sensitive materials to form needle tips or by enclosing pH-responsive materials-based nanocarriers within the MNs. The pH-responsive MNs are typically prepared using pH-sensitive components, which include the following (Figure 3A):

The first type is sodium bicarbonate (NaHCO_3),^[118–120] which is the key component of pH-responsive reactions (Figure 3A(i)). Under normal physiological conditions, the PLGA shell or PLGA membrane can remain intact and no drug released. The MNs containing NaHCO_3 can be stimulated by an acidic environment to produce CO_2 bubbles, which leads to the rupture of hollow microspheres or polymer membranes in the MNs and the release of the medications they are encased in.

The second types is pH-sensitive polymers and copolymers, such as albumin,^[121] chitosan,^[122] dextran,^[123,124] peptide histidine (His),^[125] oligo(sulfamethazine)-b-poly(ethylene glycol)-b-poly(β -aminoester urethane) (OSM-b-PEG-b-PAEU),^[126,127] dimethylmaleic anhydride-modified polylysine (PLL-DMA),^[128] lipid-coated NPs,^[129,130] and so on, which are released in response to changes in intermolecular forces (such as electrostatic and supramolecular interaction) caused by charge reversal. To be more precise, albumin has an isoelectric point (pI) value of 4.9. At pH values lower than its pI, albumin carries a positive charge, whereas at the physiological pH value, it has a negative charge. Albumin was used to promote pH-sensitive disintegration of PEM assembly due to its charge inversion properties in response to hydrogen concentration in the surrounding medium.^[125] The researchers chemically linked ethoxypiprene to dextran via an acid-catalyzed reaction. This resulted in a modified form of dextran, known as m-dextran, with 89% of its hydroxyl groups replaced by pendant acetals. The dextran was altered to possess an acid-responsive characteristic.^[123,124] The unsaturated nitrogen atom of the imidazole ring in His side chain possesses a lone pair of electrons. This side chain is hydrophobic when deprotonated in a medium with a pH value above 6.0, but becomes

hydrophilic when the pH is below 6.0. Thus, polymeric micelles (PMs) are made of His exhibited pH-sensitive properties. When the pH of the surrounding environment was reduced from 7.4 to 5.0, there was an increase in the release of medicines in the PMs as the pH declined.^[129] Similarly, when the MNs covered with PLL-DMA transition layers are exposed to an acidic environment, the negatively charged PLL-DMA will undergo a transformation into positively charged PLL. The transition layers would rapidly disintegrate, facilitating the swift release of the outermost medicines (Figure 3A(ii)).^[128] Besides, pH-sensitive lipid-coated NPs showed excellent pH responsiveness and well-targeting properties.^[129,130] Host-guest supramolecular vesicles formed by pillar[n] arenes with many guest compounds are also utilized as pH-responsive MNs preparation materials due to their reversible pH-responsiveness.^[131]

The third class of materials undergoes phase transitions (expansion or degradation) as pH changes. For example, the hydrogen evolution reaction (HER) is a reduction process that leads to an elevation in the pH level at the electrode's vicinity. Applying the aforementioned approach, the HER was enforced at the MN array, causing an elevation in the pH level. This, in turn, would result in the expansion (and potential dissolution) of the needle structure made of cellulose acetate phthalate (CAP) polymer.^[132] In addition, ZnO quantum dots (ZnO QDs) exhibit unique acid degradation characteristics, undergoing rapid degradation when exposed to acidic conditions with a pH below 5.5, but remaining stable or degrading slowly under physiological conditions ($\text{pH} \approx 7.4$). This property makes them suitable for acting as “gatekeepers” to seal the nanopores of drug carriers, preventing drug leakage and enabling the release of preloaded drugs in an acidic environment.^[133] Researchers utilized this idea to develop and utilize pH-responsive MNs for controlled medication release (Figure 3A(iii)).^[134] In addition, pH-sensitive zeolitic imidazolate frameworks-8 (ZIF-8), which consist of 2-methylimidazolate and Zn^{2+} ions, is a significant subgroup of MOFs. ZIF-8 exhibits susceptibility to degradation in a regionally acidic setting while demonstrating robust stability in a neutral setting. Thus, ZIF-8 has been employed for the purpose of regulating the release of medications in the treatment of cancer or diabetes.^[135]

These smart MNs have the ability to regulate the administration of medications based on the fluctuations in the body's pH levels. This capability can enhance the efficacy of treatment and mitigate the extent of systemic toxicity to some extent. However, pH-responsive MNs impose high requirements on the stability and chemical properties of the loading drugs. In addition, the gradient of pH value change in skin tissue is often small, and the precise “on-off” controlled release effect in a narrow pH value window requires extremely high requirements for material and structure design.

2.2.2. Glucose-Responsive MNs

The 9th edition of the International Diabetes Federation Diabetes Atlas 2019 reports that there are over 536.6 million adults globally who have diabetes. It is projected that this figure will increase to 783.2 million by the year 2045.^[136] Insulin therapy is crucial for controlling BGLs in individuals diagnosed with diabetes.^[137] Nevertheless, the frequent surveillance of BGLs and the

Table 2. Summary of endogenous stimulus-responsive MNs on biomedical treatment.

Stimuli	Responsive compositions	Applications	Drugs	Animal models	References
pH	NaHCO ₃ Albumin, pyridine groups, <i>m</i> -dextran, His, OSM- <i>b</i> -PEG- <i>b</i> -PAEU, dimethylmaleic anhydride-modified polylysine, cholesterol, pillar[5]arene	transcutaneous on-demand controlled release drugs, antihypertension DNA vaccination for Alzheimer's disease, Dermal Vaccination of IPV, Cancer immunotherapy, Obesity Treatment, Psoriasis treatment, Gene therapy for subcutaneous cancer, Head and Neck Cancer chemotherapy, Synergistic antitumor effects of immuno-chemotherapy, diabetes therapy	Alexa 488, Cy5, calcein, nifedipine, diltiazem IPV, aPD1, anti-CTLA-4, Rosiglitazone, CL 316243, SKN, Plasmid DNA, pOVA, poly(I:C), p53 DNA, Cisplatin, aPD1, Insulin	cadmium chloride-induced hypertension rats B16F10 mouse melanoma model, diet-induced obese mice, IMQ-induced mice, Alzheimer's disease mice models, lung metastasis tumor model, subcutaneous tumor model, xenograft head and neck tumor model using FaDu cells immunocompetent murine tumor homograft model, STZ-induced diabetic SD rats	[118–120] [121–131]
Glucose	cellulose acetate phthalate, ZnO QDs, ZIF-8 GOx PBA, 3-(acrylamido)PBA, 4-carboxy-3-fluorophenylboronic acid-grafted e-polylysine, (4-((2- acrylamidoethyl) carbamoyl)-3-fluorophenyl)boronic acid, 3-aminophenylboronic acid, 4-(2-acrylamidoethylcarbamoyl)-3-fluorophenylboronic acid, ZnO-PBA-2, 4-acrylamido-3-fluorophenylboronic acid	electrochemically controlled drug release, Diabetes therapy Treatment of diabetes Treatment of diabetes, Hypoglycemia Prevention and therapy	Toluidine Blue, insulin Insulin Insulin, glucagon	STZ-induced diabetic SD rats STZ-induced type 1 diabetic mice STZ-induced diabetic SD rat, mice and minipig	[132, 134, 135] [131, 135, 152] [144–151, 153–157]
Insulin	insulin aptamer	Hypoglycemia Prevention	glucagon	STZ-induced T1D mice	[160]
ROS	thioketal, HA, PLA-mPEG, PVA, PLGA	Psoriasis Therapy, Periodontal Disease Treatment	Methotrexate prodrug, Metronidazole	IMQ-induced psoriatic mouse model, periodontitis rat model	[174, 173]
H ₂ O ₂	mPEG- <i>b</i> -P(Ser-PBE), poly(phenylboronic acid pinacol ester), 4-(imidazolyl carbamate)phenylboronic acid pinacol ester, MPEG- _{3K} -P(DMAEMA-PBA) _{HK}	Treatment of diabetes	Insulin	STZ-induced diabetic SD rats	[169–172]
GSH	PEG- _{3K} -Cy5 ₄ -L ₈ -CA ₈	multidrug-resistant ovarian cancer treatment	betulinic acid, paclitaxel	Orthotopic multidrug-resistant ovarian cancer model	[178]
HAase	<i>m</i> -HA, HA-NPs	The treatment of melanoma through synergistic immunotherapy strategy	aPD1, 1-MT	B16F10 mouse melanoma model	[182]
Thrombin	HA, thrombin cleavable peptide, MBA	auto-regulation of blood coagulation	HP	Thrombotic challenge model	[183]
Bacterial enzyme	PCL, Poloxamer 407, AdminPen devices	antimicrobial	CAR	Skin wound model	[185]
Bacterial lipase	PVP, PVA, PCL, Poloxamer 407, Gantrez S-97	Management of infected chronic wounds	CAR	ex-vivo neonatal porcine skin wound infection model	[184]
Lipolytic esterase	PVP, PVA, PCL, AgNO ₃	improved treatment of biofilm skin infection	silver NPs	ex vivo biofilm model in rat skin	[186]
Endogenous temperature	pNIPAM hydrogel	Wound management	Human VEGF/EGF, mupirocin	Diabetic mice wound model, full-thickness skin wounds of a mouse model, severe infected wound model	[190–192]

The Response Mechanism of Endogenous Stimulus-Responsive MNs

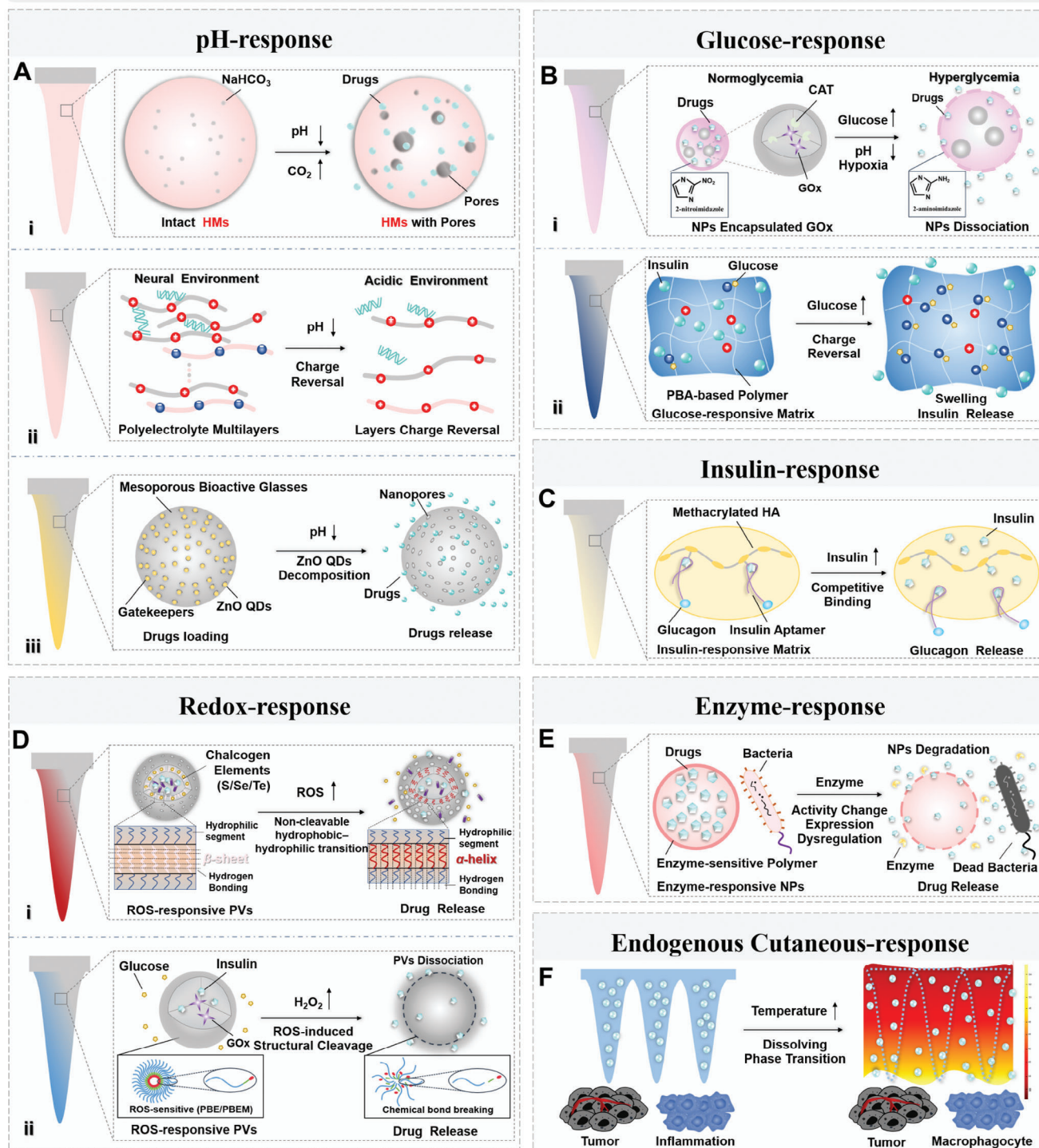


Figure 3. Schematic of the responding mechanism of different endogenous stimulus-responsive microneedles. A) pH-sensitive components are commonly used to prepare pH-responsive MNs. i) The acidic environment stimulates the MNs containing NaHCO₃ to generate CO₂ bubbles, which rupture the hollow microspheres or polymer membrane in the MNs, thereby releasing the encapsulated drugs. Reproduced with permission.^[118] Copyright 2012, Elsevier. ii) Changes in intermolecular forces (such as electrostatic and supramolecular interaction) caused by charge reversal result in structural changes in pH-sensitive polymers and copolymers that promote drug release. Reproduced with permission.^[128] Copyright 2019, Elsevier. iii) As pH changes, the material undergoes a phase transition (expansion or degradation). For instance, ZnO quantum dots (ZnO QDs) have peculiar acid degradation properties, which can be used as “gatekeepers” to cap the nanopores of drug carriers to prevent drug leakage and allow preloaded drugs to be released in an acid environment. Reproduced with permission.^[134] Copyright 2018, American Chemical Society. B) Drug release mechanisms in glucose-responsive

conventional subcutaneous administration of insulin in individuals with diabetes are frequently associated with discomfort, inadequate glycemic control, low adherence, and other complications. The implementation of MNs technology has the potential to enhance the management of diabetes in a manner that is both painless and convenient for patients. However, the regular management approach of typical medical nurses cannot be automatically adapted to the fluctuation of blood glucose levels. This poses potential dangers including inadequate treatment, kidney failure, vision loss, low blood sugar, brain damage, cognitive impairments, and seizures.^[138,139] In recent years, researchers have focused on developing a closed-loop drug delivery strategy for diabetes, also known as a self-regulated drug delivery strategy. This approach aims to intelligently control the dynamics of drug release based on the fluctuation of blood glucose levels. It has shown significant potential in the treatment of diabetes by addressing the aforementioned problems.^[140] Glucose-responsive MNs that contain insulin or glucagon serve as an “artificial pancreas” by keeping BGLs within the normal physiological range. These MNs are highly suitable for a closed-loop glycemic management system.

To develop self-regulated MNs delivery systems that respond to blood glucose concentration, the most commonly used glucose-sensitive principles are: i) the glucose oxidase (GOx)-based enzymatic reaction; ii) boronic acid-containing polymers construct glucose-sensitive materials; iii) the infrequently utilized glucose-binding proteins like concanavalin A (Con A). The above work principles of glucose-responsive MNs are introduced as follows in detail.

GOx-Based Glucose-Responsive MNs: During a hyperglycemic condition, GOx has the ability to transform glucose into gluconic acid in the presence of oxygen. This process leads to the creation of an acidic, hypoxic, and hydrogen peroxide (H_2O_2)-rich microenvironment in the immediate vicinity.^[141] Based on the GOx-mediated enzymatic reaction and a series of changes, researchers designed the related glucose-responsive MNs.

In the past decades, MNs designed with the changes of glucose oxidation reaction products as stimulus signals emerge in an endless stream. Some studies immobilized GOx and/or catalase (CAT) in MNs made of pH-responsive materials (such as $NaHCO_3$, ZnO QDs, dextran, ZIF-8, host–guest supramolecular vesicles, etc.) that encapsulated drugs.^[123,124,131,133–135] For example, In order to create hybrid functional materials that can be employed as drug carriers, Xu et al.^[134] effectively combined the pH sensitivity of ZnO QDs with the porous structure of mesoporous bioactive glasses (MBGs) (Figure 3A(iii)). The glucose-responsive factor, consisting of GOx and CAT, is encapsulated

within MBGs. This factor catalyzes the conversion of glucose into gluconic acid, resulting in a localized reduction in pH and the dissolution of ZnO QDs. Subsequently, this led to the formation of nanopores on MBGs and the subsequent liberation of the enclosed insulin. Nevertheless, the buffering impact of the internal environment may result in a lack of promptness in the pH alteration process, leading to a delay or lag in the release of the drug.^[142] Comparatively speaking, the glucose oxidation process consumed oxygen and rapidly formed a local anoxic environment. Therefore, hypoxia had the advantage of rapid response as a stimulus signal to control drug release. Some researchers immobilized GOx in insulin MNs made of hypoxia-sensitive materials (such as amine-functionalized 2-nitroimidazole (NI) groups). Researchers have utilized the occurrence of hypoxia in the immediate vicinity caused by the consumption of oxygen in the enzymatic reaction as a stimulus for prompt insulin release in response to high blood sugar levels. In order to develop transduction that responds to hypoxia, glucose-responsive micro/NPs were created. These MNs are made up of vesicles that are responsive to glucose (GRVs) and contain insulin and GOx. The GRVs are formed from HA that is sensitive to hypoxia and coupled with hydrophobic NI that has amine functionality. During hyperglycemia, the enzymatic oxidation of glucose creates a local hypoxic milieu. This leads to the reduction of NI groups on the HS-HA into hydrophilic 2-aminoimidazoles. As a result, the GRVs dissociate quickly and release insulin (Figure 3B(i)).^[142,143] Others immobilized GOx in insulin MNs made of H_2O_2 -sensitive materials (See “2.2.4.1 Oxidation-responsive MNs” for details).

Overall, safety concerns related to GOx can hinder its extensive use due to factors such as limited tolerance for prolonged usage, protein denaturation during storage, the production of toxic byproducts through glucose reactions, and its rapid response to hyperglycemia conditions, leading to a lack of sustained release. Hence, there is a pressing requirement for medication delivery techniques that can provide enhanced, accurate, and efficient healthcare, while circumventing the aforementioned issues. This necessitates the study and innovation of new materials, novel designs, and innovative architectures.

Glucose-Responsive MNs Based on Boronic Acid-Containing Polymers: Compared with protein-based glucose-sensitive elements, glucose-responsive MNs constructed from polymers containing boronic acid have unique advantages, such as low toxicity, stability, reversible bonding, ease of modification, and so on. One typically utilized type is PBA which contains electron-withdrawing moieties. The glucose response is really caused by a glucose-dependent change in the balance of the PBA molecule, shifting between its uncharged and anionically charged boronate

MNs. i) Based on the GOx-mediated enzymatic reaction and a series of changes, glucose-responsive MNs for drug release were designed. Reproduced with permission.^[143] Copyright 2015, National Academy of Science. ii) Drug release mechanism of glucose-responsive MNs based on boronic acid-containing polymers. Reproduced with permission.^[146] Copyright 2020, Springer Nature. C) Taking high insulin concentration as the stimulus signal of glucagon control release, when the insulin concentration increased, the competitive binding between free insulin and immobilized insulin on HA realized the rapid release of glucagon on demand, thus preventing the risk of hypoglycemia. Reproduced with permission.^[160] Copyright 2017, WILEY. D) The drug release mechanisms of ROS-responsive MNs involve changes in polymer solubility from hydrophobic to hydrophilic characteristic (i) or ROS-induced chemical bond cleavage (ii). Reproduced with permission.^[168] Copyright 2018, Elsevier. E) The enzyme-responsive drug delivery carrier was designed by utilizing the unique microenvironment of high expression of bacterial lipase at the site of bacterial infection. With enzyme activity change or expression dysregulation, the enzyme-sensitive polymer degrades, thus promoting the release of antibiotics. F) Changes in skin temperature caused by diseases such as inflammation/cancer/wounds act as an endogenous stimulus that promotes the on-demand delivery of drugs by cutaneous thermo-responsive MNs.

forms. A glucose-responsive transdermal medication delivery approach was developed based on the PBA-based polymer/MN hybrid system. Under hyperglycemic conditions, the reversible formation of a glucose-boronate complex causes an increase in negative charges in the polymeric matrix. This leads to increased swelling of the MNs and weakens the electrostatic interactions between negatively charged insulin and polymers. As a result, insulin diffuses rapidly into the subcutaneous tissue (Figure 3B(ii)).^[144–147] More inventively, insulin was grafted onto the molecules of PBA derivatives to create molecules that release insulin in response to glucose.^[148,149] More glucose molecules competed with the boronate species at greater glucose concentrations, causing the MNs to produce more insulin. Additionally, at euglycemia, the PBA-2 grafted ZnO dots (ZnO-PBA-2) were used as the “gate keepers” to prevent insulin from evaporating from the mesoporous silica NPs (MSNs). However, the link between PBA-2 and the gluconamide connected to the MSN was severed during hyperglycemia to aid in the release of insulin.^[150] In contrast to earlier insulin delivery systems based on PBAs, the Wulff-type PBA was initially employed as the glucose-responsive linker in the aforementioned insulin delivery system. This method successfully achieved both sustained management of BGLs and prevention of hypoglycemia. A different approach involves the copolymerization and crosslinking of PBA-derived monomers and auxiliary monomers to create hydrogel-based MNs that are responsive to glucose. Typically, the change in counterionic osmotic pressure leads to a change in the hydration of the gel. This causes localized dehydration of the gel surface, also known as the “skin layer”. As a result, the diffusion of insulin loaded in the gel is controlled.^[151–153] Using a novel approach, glucose-responsive microgels containing 4-acrylamido-3-fluorophenylboronic acid (AFBA) units undergo mono-complexation with glucose when exposed to high or normal blood sugar levels, resulting in the swelling of the microgels. When glucose levels are low, the AFBA unit causes secondary crosslinking between polymer chains, leading to significant shrinkage of the microgel. Ultimately, the preloaded glucagon was expelled from the microgels and promptly discharged from the MNs.^[154] By combining glucagon microgel with poly(methyl vinyl ether-alt-maleic anhydride) and poly(ethylene glycol) (PEG), followed by thermal cross-linking, Lu et al.^[155] created a smart glucagon MN using the same technique. The glucose-responsive mechanism of the insulin and glucagon dual-delivery MNs patch relies on the combined effect of the AMH/APBA polymeric network's net charge shift, which varies with glucose concentrations, the difference in pI of insulin and glucagon at normal pH levels, and the resulting contraction or expansion of the surrounding polymeric gel matrix.^[156] Moreover, recent advancements have demonstrated that gold nanoclusters modified with PBA derivatives exhibit glucose-responsive behavior as nanocomplexes. These nanocomplexes can be used to create smart MNs with excellent drug-loading capability, favorable biocompatibility, mechanical strength, and little toxicity when tested in living organisms.^[157]

In conclusion, several techniques were used to create glucose-responsive MNs materials, including one-step grafted modification, graft copolymerization, surface coating, generating porous structure, employing silk fibroin (SF), combined semi-

interpenetrating network (semi-IPN) hydrogel, and sequential photopolymerization preparation strategy.

2.2.3. Insulin-Responsive MNs

Insulin replacement therapy is crucial for individuals diagnosed with type 1 and severe type 2 diabetes.^[158] Intensive insulin therapy can enhance blood glucose control and decrease the likelihood of long-term problems, particularly in individuals with type 1 diabetes.^[159] Nevertheless, the regular administration of insulin doses and boluses, whether through injections or subcutaneous insulin infusion, can heighten the likelihood of experiencing hypoglycemia. Hence, utilizing a high quantity of insulin as the stimulus signal for regulating the release of glucagon holds clinical value in the prevention of hypoglycemia. Yu et al.^[160] devised a method for administering glucagon triggered by insulin using an MN-array patch to prevent hypoglycemia, following this procedure. As shown in Figure 3C, insulin aptamer consisted of a single-stranded oligonucleotide with a unique secondary structure. The insulin aptamer was conjugated with glucagon and subsequently bound to immobilized insulin on methacrylated HA (m-HA) through the particular interaction between the insulin aptamer and the target insulin. This resulted in the creation of an insulin-responsive m-HA matrix. The glucagon smart micro-needles were created by utilizing insulin-responsive m-HA as the matrix material. As the concentration of insulin grew, the interaction between free insulin and immobilized insulin on HA resulted in the prompt release of glucagon when needed, effectively averting the occurrence of hypoglycemia. The utilization of aptamers in this controlled release method can also be expanded to encompass additional closed-loop therapeutic delivery systems for the treatment of various ailments.^[29]

2.2.4. Redox-Responsive MNs

REDOX reaction in vivo is a common biochemical process, including REDOX reaction produced in the process of cell metabolism, antioxidant system to combat oxidative stress, and so on. In these processes, different types of oxidized and reduced substances are involved, such as oxidized ROS, reduced GSH, and so on. According to the REDOX reactions and products in vivo, oxidation-responsive MNs and reduction-responsive MNs can be designed.

Oxidation-Responsive MNs: Oxidation is very common in living organisms, especially under pathological conditions. The oxidizing molecules that receive the most focus are referred to as ROS. ROS, or reactive oxygen species, refers to a collection of oxygen-containing molecules that are chemically active. These include H_2O_2 , superoxide, superoxide radical anion, hydroxyl radical, hypochlorite, and peroxynitrite.^[161,162] ROS have both positive and negative effects on many biological processes.^[163] Low-level ROS have a crucial physiological function in cell signal transduction, cell proliferation, hormone synthesis, inflammation regulation, and other biological processes.^[164] Elevated quantities of ROS in cells, in abnormal situations, result in oxidative stress and subsequent malfunction. The occurrence of this pathological alteration has been associated with

the development of cancer, inflammation, and cardiovascular illness, as well as neurodegenerative conditions like Alzheimer's disease and Parkinson's disease. Research has demonstrated that the majority of cancer cells have levels of ROS that are 100 times greater than those found in healthy cells.^[165] Thus, the use of oxidizing molecules (such as superoxide radicals, H_2O_2 , etc.) as trigger agents can lead to oxidation or structural change of MNs materials, triggering responsive behavior of materials, so as to achieve drug release or other functions in a state of stress. ROS-responsive materials commonly consist of polymers that contain chalcogen elements such as sulfide, selenide, and telluride. Other types of ROS-responsive polymers include thioether, diselenide, poly(thioether), arylboronic acid/ester-containing polymers, aminoacrylate, oligopropylene, and peroxalate ester-containing polymers.^[166] The drug release mechanisms of these polymers are based on the transition of polymer solubility from hydrophobic to hydrophilic properties (Figure 3D(ii)) or the breaking of chemical bonds generated by ROS (Figure 3D(iii)).^[167,168]

Out of all the naturally occurring ROS, H_2O_2 is regarded as the most crucial one. H_2O_2 serves multiple roles in the body and is involved in numerous physiological and pathological processes. Specifically, the concentration of H_2O_2 is significantly elevated in the tumor microenvironment (TME) compared to normal cells/tissues, which is a distinctive feature of tumors. The phenylboronic ester (PBE) is the predominant "ROS trigger group" used in ROS-responsive MNs. Under physiological settings, H_2O_2 can cause degradation of the PBE. The researchers have developed H_2O_2 -responsive PVs, MSNs, or nano-sized complex micelles (NCs) combined with MNs patches for intelligent insulin administration, following this approach.^[169–172] To prepare H_2O_2 -sensitive PVs, Hu et al.^[169] used a solvent evaporation technique to produce the self-assembled diblock copolymer mPEG-b-P(Ser-PBE). The PVs possessed hollow spherical architectures, wherein the inside was encased with insulin and GOx enzyme. Under normal physiological settings, the copolymer mPEG-b-P(Ser-PBE) undergoes a process where its PBE side chains are removed in the presence of H_2O_2 , resulting in the copolymer becoming soluble in water. This causes the disassembly of the PVs and the consequent release of insulin. In a similar manner, Tong et al.^[170] developed an insulin delivery device that responds to both glucose and H_2O_2 . They achieved this by modifying the PVs with certain functional groups, PBA for glucose sensitivity and PBE for H_2O_2 sensitivity. Furthermore, Xu et al.^[171] created MSN that are capable of responding to H_2O_2 by modifying them with 4-(imidazolyl carbamate) phenylboronic acid pinacol ester. The glucose oxidation reaction was catalyzed by GOx, which was encapsulated in MSN. This reaction produced H_2O_2 , which then oxidized the PBE located on the surface of MSN. As a result, the host-guest complexation was disrupted. This could result in the disassembly of the drug-loaded MSN and the subsequent release of insulin. Zhang et al.^[172] designed NCs with the ability of H_2O_2 and pH cascade response to participate in the formation of a bioresponsive MN-array patch for insulin delivery. Under the condition of hyperglycemia, the enzymatic reaction caused changes in local pH and H_2O_2 , which led to the destruction of the micelle structure and promoted the release of insulin.

Furthermore, the ROS-responsive linker thioketal (TK) is often used to design ROS-responsive prodrugs.^[173,174] TK is sensitive to

a range of ROS such as superoxide, H_2O_2 , hypochlorite, peroxytrite, and hydroxyl radical.^[175] Zhou et al.^[174] produced a prodrug of methotrexate (MTX) that is responsive to ROS and conjugated with HA. This was achieved by utilizing TK as the linker through an amide condensation reaction. Psoriatic lesions exhibit an overproduction of ROS by hyperproliferative keratinocytes. By applying ROS-responsive MNs to these lesions, we can trigger the release of MTX, a medication that specifically targets keratinocytes by CD44-mediated delivery. Additionally, Song et al.^[173] also developed ROS-responsive detachable MNs filled with metronidazole to transport medications into the gingival sulcus to battle anaerobic bacteria for treating periodontitis, drawing inspiration from the separable sting bee. In this study, in order to allow the MNs to react to the high ROS situation in the infected gingival sulcus, unlock the tips through ROS, and release metronidazole directly into the gingival sulcus, defeating the bacteria, a ROS-responsive polymer (PLGA-TK-PEG) was used as the MN tips in this study. In the rat periodontitis model, these MNs showed exceptional effectiveness in anti-bacterial and bone loss inhibition. Additionally, a boronate moiety was added to an anticancer medication to create a ROS-responsive prodrug, which lessens the deleterious toxicity of the drug to healthy cells and tissues before ROS activation.^[176]

Reduction-Responsive MNs: According to studies, the concentration of intratumoral GSH is 7–10 times that of normal cells, and the concentration of intratumoral GSH is ≈ 2 –10 mM, ≈ 1000 times that of the extra-tumoral environment (2–10 μ M).^[177] Due to the presence of high intracellular GSH, reducible disulfide bonds are suitable for establishing a GSH-responsive drug delivery system. Qu et al.^[178] created a programmed-response crosslinked micelle by including PEG^{SK}-Cys₄-L₈-CA₈, which effectively generated disulfide crosslinks within the micelle in response to the high levels of GSH found in tumor microenvironments. The treatment outcomes have verified that the controlled and targeted release of anticancer medications at the tumor sites has successfully suppressed the progression of multidrug-resistant (MDR) ovarian cancer and enhanced the effectiveness of the therapy for MDR ovarian cancer.

2.2.5. Enzyme-Responsive MNs

Enzymes have a vital function in regulating cells, making them significant targets for the development and treatment of drugs.^[179] Enzyme activity or expression dysregulation is the pathological basis of many diseases. In therapeutics, abnormal regulation of enzymes is a promising biological trigger.^[180,181] Studies on enzyme-responsive MNs have made significant advancements, demonstrating considerable promise in the diagnosis and treatment of cancer and other medical conditions. Ye et al.^[182] created a drug delivery system using hyaluronidase (HAase) that is activated in the tumor microenvironment. This system enhances the immune response against tumors by combining the checkpoint blockade of programmed cell death protein 1 (PD1) and indoleamine 2,3-Dioxygenase (IDO). The high level of HAase in the tumor area promoted the decomposition of the nanovesicles, which in turn released anti-PD1. Researchers utilized a B16F10 mouse melanoma model to illustrate that the combined administration of anti-PD1 (aPD-1) and 1-methyl-DL-

tryptophan (1-MT) resulted in a robust and enduring suppression of tumor growth. This study presented a strategic approach to effectively counteract the immune evasion mechanisms by eliciting a robust antitumor immune response.

In addition, Zhang et al.^[183] developed a polymer-drug patch that responds to thrombin. They achieved this by attaching heparin to the main chain of HA using a thrombin-cleavable peptide (GGLVPR | GSGGC). This created a closed-loop system for regulating anticoagulant activity in a sustainable manner. The thrombin-responsive HP conjugated HA (TR-HAHP) matrix enabled the MNs to promptly react to increased thrombin levels, resulting in the release of heparin from the matrix, which effectively prevents thrombosis. No heparin was released without thrombin, which minimized the risk of undesirable spontaneous hemorrhage.

In addition, researchers developed infection-responsive drug delivery carriers to address the issue of antibiotic resistance. They utilized the distinctive microenvironment present at the location of bacterial infection, including the elevated expression of bacterial lipase (Figure 3E).^[184–186] Specifically, Mir et al.^[184] employed dissolving MNs to transport the NPs to the infection site. The NPs were made from a bacterial lipase-sensitive polymer called PCL using a straightforward nanoprecipitation method. Besides, Permana et al.^[186] entrapped silver NPs derived from green tea extract within chitosan-decorated PCL microparticles that exhibit responsiveness. The PCL utilized in this investigation can undergo degradation by lipase enzymes synthesized by *Staphylococcus aureus* (*S. aureus*) and *Pseudomonas aeruginosa* (*P. aeruginosa*). The integration of silver NPs into PCL microparticles resulted in the specific release of silver NPs when exposed to bacterial cultures that form biofilms. This could potentially facilitate targeted delivery exclusively at the site of infection and enhance the efficacy of biofilm targeting in skin wound infections.

2.2.6. Endogenous Cutaneous Thermo-Responsive MNs

The temperature of the skin surface typically varies between 33 and 37 °C in its normal state, with variations observed in different locations. Nevertheless, in certain instances, such as in the presence of a cut, inflammation, or cancer, the typical temperature of the skin may be disrupted. Thus, alterations in skin temperature resulting from specific disorders can serve as a potent internal trigger for the targeted administration of medications using MNs in a responsive manner (Figure 3F). Persistent non-healing skin wounds can result in discomfort, inflammation, bacterial infection, and potentially even mortality, thus posing a significant risk to human well-being.^[187] Temperature is strongly correlated with the inflammatory and infectious condition of a wound. Abnormal fluctuations in wound temperature might serve as an early indicator of infection.^[188,189] Based on the temperature-sensitive swelling phase transition behavior of NIPAM hydrogel, a series of smart MNs drug delivery systems for wound management were designed.^[190–192] When infection occurred, an increase in temperature in the wound area surpassed its LCST, causing the NIPAM hydrogel to shrink, thereby releasing the encapsulated therapeutic drugs.

The main difficulty for this type of temperature-responsive magnetic NPs lies in creating and advancing thermos-responsive

materials that are both safe and sufficiently sensitive to detect small temperature variations around the standard physiological temperature of 37 °C. Besides, researchers need to pay more attention to the development of new biodegradable temperature-sensitive polymer materials and make them to the trend of multifunctional, ecological, and popular.

The human body undergoes ongoing physiological and pathological changes, resulting in significant variations in the biochemical indicators among individuals. Therefore, there are challenges in the accuracy and sensitivity of dose regulation for stimulus-responsive MNs based on changes in endogenous signals of the body. Essentially, the complexity of the design and preparation of stimulus-responsive MNs also limits the clinical application and transformation of such MNs systems. In conclusion, future research work should pay more attention to the mechanism research of the feasibility and convenience of bioreponsive MNs in the actual clinical application scenario.

2.3. Preparation Methods of Stimulus-Responsive MNs

The choice of MNs manufacturing technology or method depends on the MNs type, geometrical morphology, materials, and responding mechanism.^[193] The stimulus-responsive MNs are often fabricated using traditional MNs preparation techniques, such as micromolding, etching, spray coating, drawing lithography, photopolymerization, and so on.^[194] Among them, micromolding is the most widely used MNs manufacturing technology, which has the advantages of low cost and simple operation, but the manufacturing process is time-consuming and laborious with many steps, which is not convenient for mass production.^[14] 3D printing technology has gradually become a promising method for MNs preparation. This technique makes it possible to fabricate MNs arrays with different geometric forms. However, low resolution, slow fabrication rate, rough surface, and limited material options limit the practical application of this technique.

In addition to conventional techniques, the researchers can also prepare the stimulus-responsive MNs using an electrochemical deposition method, reverse-phase microemulsion molding method, dip-coating process, LBL assembly, LBL coating, chemical modification with sensitive surface groups (such as pyridine-modified), double-emulsion method to prepare MNs materials with given response properties.^[12,49,87,122] In brief, the preparation of stimulus-responsive MNs is complex and challenging. With the development of new materials and the improvement of MNs functional requirements, emerging MNs manufacturing processes continue to emerge, which will promote the reform of smart MNs.

3. Stimulus-Responsive MNs-Mediated Cancer Therapy

Nowadays, cancer is indeed one of the most life-threatening diseases in humans and an important obstacle to improving life expectancy.^[195,196] In clinical treatment, the commonly used anticancer treatment strategies include chemotherapy, surgery, and radiotherapy. Nonetheless, for various reasons, the antitumor efficacy of this treatment is still insufficient: 1) surgical treatment

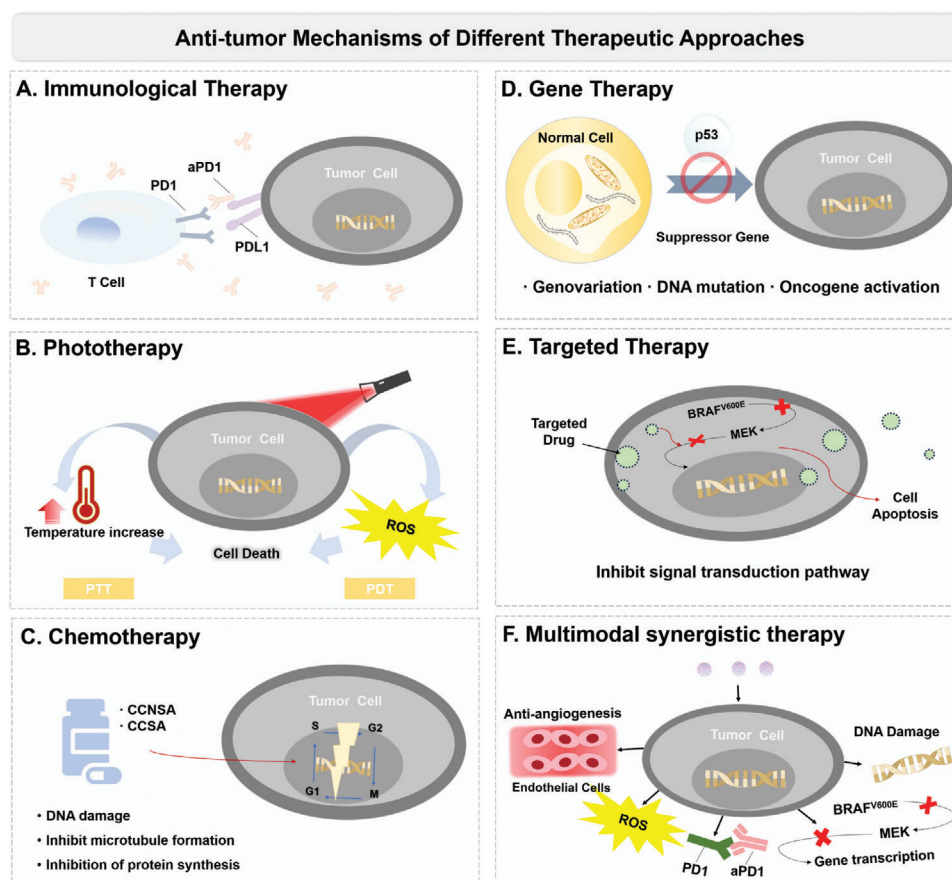


Figure 4. Schematic of the therapeutic mechanisms of different anti-tumor therapies, including A) immunological therapy, B) phototherapy, C) chemotherapy, D) gene therapy, E) targeted therapy, and F) multimodal synergistic therapy.

is invasive and may be accompanied by postoperative complications and postoperative recurrence; 2) Some patients are diagnosed with advanced cancer and lose the opportunity for surgery; 3) The side effects of systemic application of chemotherapeutic drugs hinder their use; 4) Multidrug resistance to chemotherapeutic drugs is becoming more common; 5) Radiotherapy damages the physiological state of normal tissues. The limitations of conventional cancer treatment methods can significantly impact the quality of patients' life and are no longer entirely sufficient to meet the demands of clinical treatment.^[197] As research into anti-tumor therapies continues to advance, new therapy strategies such as immunotherapy, phototherapy, local delivery of chemotherapeutic drugs, gene therapy, and targeted therapy are developing rapidly.

Figure 4 illustrates the main mechanisms of action of these antitumor therapies. Currently, the main strategy of tumor immunotherapy is to enhance the immune killing effect of T cells by using the competitive binding of immune checkpoint inhibitors (e.g., anti-PD-1, anti-PD-L1, anti-CTLA-4), restore the body's immunity, and thus exert anti-tumor effects (Figure 4A). In addition, cancer phototherapy can exert anti-tumor efficacy through the local thermal ablation effect of PTT or ROS generation by PDT to kill tumor cells (Figure 4B). Besides, chemotherapy drugs are divided into cell cycle-specific agents (CCSA) and cell cycle nonspecific agents (CCNSA) according to their mechanism

of action. Different chemotherapeutics act at different stages of the cell cycle. Some block DNA synthesis, or inhibit microtubule formation, then arrest cell mitosis, thereby slowing or preventing tumor development (Figure 4C). Moreover, cancer gene therapy aims to inhibit the growth of cancer cells by introducing normal tumor suppressor genes or using gene editing techniques to repair damaged DNA and restore normal gene function (Figure 4D). Furthermore, in cancer-targeted therapy, drugs are used to inhibit tumor growth by interfering with specific molecular signaling pathways or targets within cancer cells (Figure 4E). Additionally, tumor synergistic therapy is the simultaneous or continuous application of numerous treatments to enhance the anti-tumor effect, increase efficacy, and decrease side effects (Figure 4F).

Combined with the above anti-tumor therapeutic mechanisms, in order to effectively deliver therapeutic drugs (such as vaccines, chemotherapeutic drugs, PSs, photothermic agents, etc.) to the tumor site to achieve anti-tumor efficacy, stimulus-responsive MNs have significant advantages in the tumor environment compared to traditional drug delivery methods, enabling on-demand, targeted drug delivery. Lately, stimulus-responsive MNs have become a hot topic in tumor therapy research. In current practices, stimulus-responsive MNs have been widely used for treating superficial tumors (skin tumors,^[54,65] head and neck cancer,^[129] breast cancer,^[56] etc.),

Table 3. Summary of the applications of stimulus-responsive MNs in cancer therapy.

Anti-tumor method	Stimuli	Tumor type	Drugs	Materials	References
Immunotherapy	pH, Glucose	B16F10 Melanoma	aPD-1	cross-linking HA, <i>m</i> -dextran	[123]
	HAase	Melanoma	aPD-1, 1-MT	<i>m</i> -HA	[182]
	pH	SCC VII-luc cells	aPD-1, CDDP	PVP	[134]
	ultra-pH	Lung metastasis tumor	Poly (I:C), DNA vaccines	OSM-(PEG-PAEU)	[127]
PDT	Light	B16F10 Melanoma	L-Ce6	oligo-HA	[54]
		Intradermal breast cancer	Ce6, sodium percarbonate	PVP	[56]
PTT	Light	A375 tumor	HPPH, CZCH	HA, CAT, Cu ²⁺ , Zn ²⁺ , HPPH	[205]
	Light	Superficial cancer	DOX, LaB ₆ @SiO ₂	PCL	[59]
		Superficial skin cancer	DOX, Gold nanocages	HA	[65]
Chemotherapy	Light	Melanoma	ICG, DOX	PVA, PATC	[206]
		squamous cell carcinoma, melanoma	ICG, 5-Fu	HA, polyethylene glycol polycaprolactone	[68]
Gene	pH	head- and-neck cancer	cisplatin	Lipid coating NPs	[130]
	pH	subdermal tumor	p53 DNA	(PLL-DMA/polyethyleneimine) ₁₂ , (p53 DNA/polyethyleneimine) ₁₆	[128]
Targeted	Light	4T1 tumor	pFBXO ₄₄	oligo-HA, PEI, LA	[210]
	Light	melanoma	Trametinib, dabrafenib	Mesoporous organo-silica NPs, PEG	[75]
	pH	ER-positive breast cancer	ERD308, Palbociclib	MPEG-poly(β -amino ester), cross-linked HA	[214]
Multimodal Synergy Therapy	Light	B16F10 tumor	Tumor lysate contains melanin	Methacrylated HA	[79]
	Light, nanozyme	melanoma	CuQGD, PdNPs	HA, PSi	[215]

ovarian cancer,^[178] and brain tumors.^[61,198] We reviewed the applications of stimulus-responsive MN in different antitumor therapies and summarized their research progress as shown in **Table 3**.

3.1. Stimulus-Responsive MNs-Mediated Immunotherapy

Cancer immunotherapy works to activate and bolster the body's immune system, enabling it to regulate and eliminate cancer cells and is often combined with other conventional treatment methods to fight tumors.^[199] Importantly, the skin, being one of the body's largest immune defenses, serves an important role in immune activation and regulation. Human skin contains a substantial number of antigen-presenting cells that possess the capability to detect, uptake, and present foreign antigens to the lymphocytes within the draining lymph nodes, thereby initiating adaptive immune responses.^[200] Therefore, the skin is an ideal site for tumor immunotherapy, especially for superficial tumors. Stimulus-responsive MNs can not only take advantage of the skin's natural immune advantages to activate the immune response, but also enable the control and deliver the anticancer drugs to tumor sites by stimulus signals. This approach enhances drug delivery efficiency while decreasing both adverse effects and costs.

For the moment, immune checkpoint inhibitors show a powerful potency in tumor immunotherapy. Among the existing studies, checkpoint inhibitors delivered by stimulus-responsive MNs mainly include aPD-1 and anti-CTLA4 (aCTLA4).^[123,182] Based on

the local acid environment of the tumor, Wang et al.^[123] prepared pH-responsive bio-degradable MNs consisting of HA and NPs encapsulating GOx/CAT and aPD-1 to realize the continuous release of aPD-1 (**Figure 5A**). The *m*-dextran was selected as the polymer matrix of NPs loaded with drugs and enzymes, which was biodegradable and had good biocompatibility. Besides, as a structural material of polymeric MNs, HA was chosen for its excellent biocompatibility and tailor-made cross-linking. In the B16F10 mouse model, the application of MNs triggered strong immune responses, resulting in substantial and sustained inhibition of tumor growth. After treatment, tumors even completely regressed in some cases. This sustained antitumor effect was associated with MNs-based delivery leading to the persistent presence of antibodies around the tumor tissue. On this basis, the researchers used MN loaded with aPD-1 and aCTLA4 to treat melanoma mice, showing a significant synergistic effect requiring only half the dose of drugs. This administration strategy can achieve the desired therapeutic effect with a relatively low dose, thereby diminishing the potential for an immunosuppressive state.

In the evolution of immune evasion, inefficient infiltration of lymphocytes has limited the clinical benefit of immunoregulation in cancer therapy. Built upon the principles of synergistic immunotherapy, Ye and colleagues developed MNs for the local targeted treatment of melanoma, using the MNs platform as a platform to cooperatively deliver immune checkpoint inhibitors 1-MT and aPD-1, with the aid of overexpressed HAase around the tumor microenvironment, to overcome the immune escape mechanism (**Figure 5B**).^[182] It was believed that 1-MT, a small

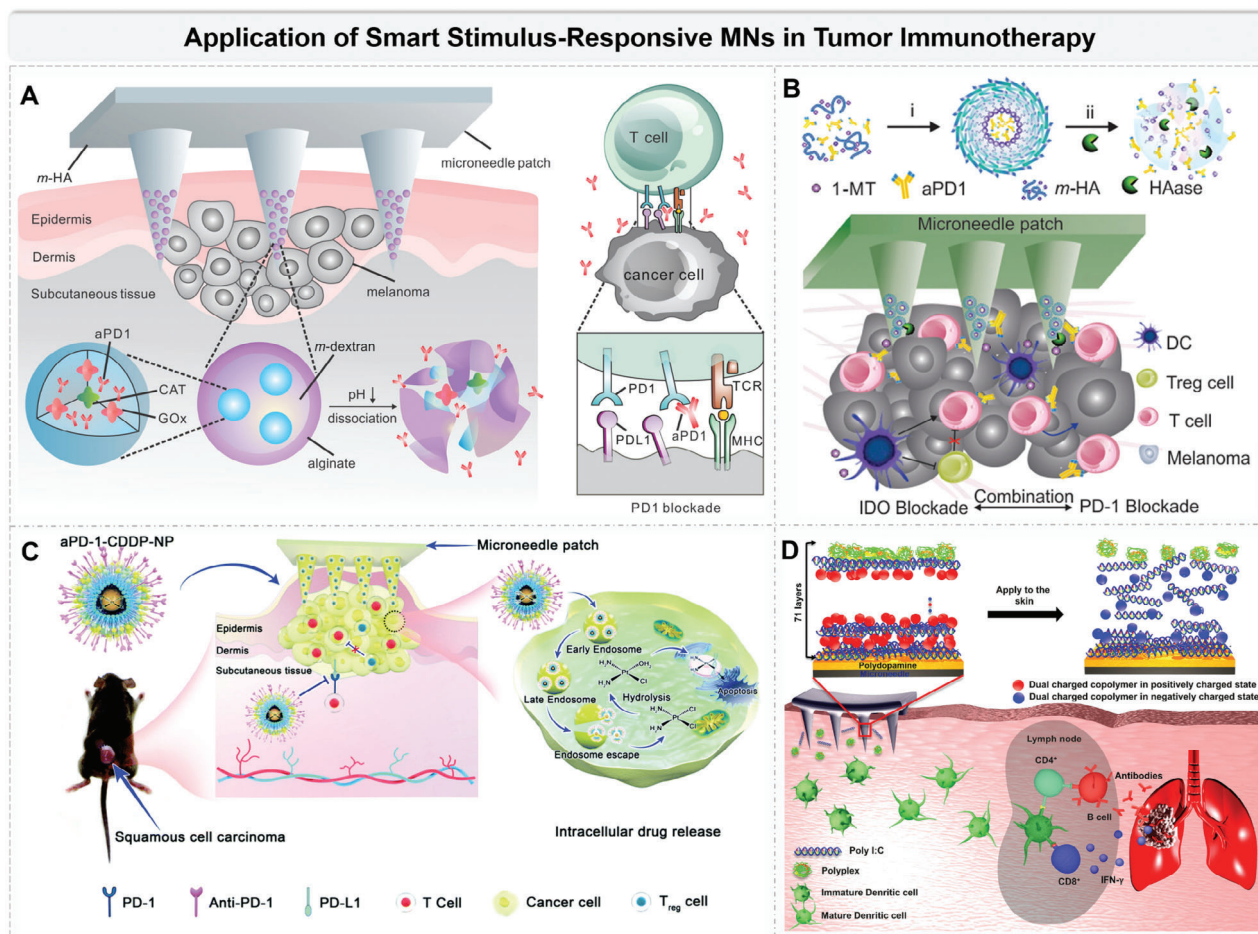


Figure 5. Stimulus-responsive MNs-mediated immunotherapy. A) Schematic of the MN patch-assisted delivery of aPD1 for skin cancer treatment. Reproduced with permission.^[123] Copyright 2016, American Chemical Society. B) Schematic illustration of the therapeutics delivery using microneedles and the enhanced immune responses at the skin tumor site. Reproduced with permission.^[182] Copyright 2016, American Chemical Society. C) Schematic illustration of the synergistic effects of immuno-chemotherapy delivered through a microneedle. Reproduced with permission.^[130] Copyright 2020, Royal Society of Chemistry. D) Schematic illustration of controlled delivery nanoengineered DNA vaccine from microneedles (MNs) assembled with LbL coating of ultra-pH-responsive OSM-(PEG-PAEU) and immunostimulatory adjuvant poly(I:C). Reproduced with permission.^[127] Copyright 2018, Elsevier.

molecule released from *m*-HA, could block immuno-inhibitory pathways in the tumor environment. In the meantime, increased numbers of alloreactive T cells were accompanied by subsequent release of aPD-1 that blocked PD-1. A significant feature of the system was biocompatibility and low cytotoxicity. There was no evidence of toxicity or inflammation in major organs such as skin, colon, liver, kidney, lungs, and intestines after histopathology was conducted on the samples.

To increase immune response rates and overcome drug resistance, Lan and colleagues described MNs loaded with pH-sensitive, tumor-targeted lipid NPs, which can precisely transport cisplatin (CDDP) and aPD-1 to tumor tissues for cancer therapy (Figure 5C).^[130] The researchers selected PVP as the MNs structure material and prepared dissolving MNs by molding method, which could be dissolved in the skin of mice within 20 min. In a mouse tumor homograft model with immune function, MNs loaded aPD-1/CDDP@NPs significantly inhibited tumor growth, augmented the quantity of activated T-cells, and effectively eradicated tumor cells. By activating the anticancer synergistic mechanism, the treatment can effectively improve the body's immune

response and significantly reduce the tumor burden. In addition, the systemic toxicity and side effects of the MNs were evaluated by recording body weight, measuring serum (Blood Urea Nitrogen) BUN and total immunoglobulin G (IgG) values, and observing HE staining of major organ specimens. As a result, all organs were severely affected by CDDP, while all organs were not adversely affected by aPD-1. Using MNs for delivering aPD-1/CDDP@NPs, the toxicity of CDDP was reduced to some extent after nanoencapsulation. As a result, it was demonstrated that it is safe to deliver aPD-1/CDDP@NPs via MNs technology for the treatment of cancer.

Furthermore, MNs-mediated tumor vaccination is a novel method of cancer immunotherapy. Duong and colleagues devised a smart DNA vaccine delivery platform, employing an immunostimulatory enhancer, Poly (I:C), and ultra-pH-sensitive OSM-(PEG-PAEU) as carriers for loading DNA vaccine through LBL coating on the MNs (Figure 5D).^[127] When the MNs were penetrated into a corneous layer of mice and placed in a local acidic microenvironment, the release of DNA vaccines and adjuvants was prompted by the high-sensitive pH-responsive

characteristics of OSM-(PEG-PAEU). The liberated DNA vaccines and adjuvants facilitate dendritic cell maturation and stimulate the production of type I interferons, leading to the generation of antigen-specific antibodies. This process achieves the activation of CD8⁺ T cells and antibody-dependent cell-mediated cytotoxicity, which are crucial in killing tumor cells. In vivo investigations demonstrated that the ultra-pH-responsive MNs effectively transported adjuvant pOVA vaccine and Poly (I:C) to the epidermal region abundant in immune cells. This synergistically induced both cellular and humoral immunity, resulting in a substantial inhibition of lung metastasis in murine B16/OVA melanoma cells.

3.2. Stimulus-Responsive MNs-Mediated Phototherapy

Cancer phototherapy has garnered significant recognition as an advanced photomedicine treatment in modern oncology research.^[201] MNs-based PTT and PDT are photo-mediated therapy techniques that have emerged as prospective replacement therapies for cancer treatment. These approaches offer distinct advantages, such as improved selectivity, reduced invasiveness, and minimal side effects.^[202] In the presence of oxygen, PDT usually utilizes a non-cytotoxic PS or precursor to produce a large number of ROS under laser irradiation, inducing tumor cell death.^[203] PTT uses photothermal agents to transfer light energy into hyperthermia, resulting in thermal ablation of neighboring cells.^[204] Recently, stimulus-responsive MN-assisted PDT and PTT have brought great hope for the treatment of tumors.

Starting from the PDT strategy of tumor therapy, Bian et al.^[54] loaded carrier-free self-assembled NPs (L-Ce6 NAs) into soluble MNs patch prepared by oligo-HA, which penetrated the skin and arrived at the tumor site (Figure 6A). The needle material dissolved and released L-Ce6 NAs, which were subsequently internalized by the cancer cells. In a B16F10 melanoma xenograft model, cancer cells produced huge amounts of ROS when exposed to a 660 nm laser. As compared with the control group, tumor lesions were significantly reduced in the L-Ce6 MNs group, and they survived an average of 30 days. It also inhibited tumor growth at distant sites. Hence, the straightforward and manageable L-Ce6 MNs exhibited effective antitumor effects both near and far from the treatment site, with remarkable stability. Additionally, the PDT biosafety of L-Ce6 MNs was evaluated. MNs treatment with/without light irradiation did not significantly affect the mice's body weight, major organ indices, and biochemical indices of liver and kidney functions. This was achieved without relying on intricate carriers or the use of chemotherapeutic or immunotherapeutic drugs. Therefore, they have great potential for clinical translation and application.

The efficacy of PDT can be improved by ameliorating hypoxia in solid tumors and reducing the massive accumulation of GSH in cancer cells. Li et al.^[205] used HA MNs patches (MN-CZCH) with self-oxidizing, GSH-depleting ability, for HPPH-based repeated PDT (Figure 6B). Cell tests demonstrated that the efficiency of PDT using MN-CZCH has been significantly enhanced by the self-supply of oxygen facilitated by CAT and the depletion of GSH mediated by Cu²⁺. In the A375 tumor-bearing mouse model, the growth of tumors was greatly suppressed or completely eradicated after 15 days following a single dose of the MN-

CZCH patch. The Ki67 staining images of the MN-CZCH group exhibited suppression of tumor cell multiplication. Furthermore, the MN-CZCH group demonstrated predominant retention of HPPH at the tumor site, resulting in less systemic toxicity. Similarly, the researchers found that the various routes of CZCH administration did not cause significant damage to major organs. Compared with the intravenous injection group, biochemical indexes (ALT, AST, BUN, creatinine) of the MN-CZCH group and control group did not change much. This suggested that the MNs administration strategy can improve the biosafety of PDT.

Based on the PTT strategy, Wei et al.^[76] constructed a soluble MNs delivery system loaded with an AIEgen for melanoma treatment (Figure 6C). The NIR950-loaded polymeric micelle was prepared by nanoprecipitation and concentrated on needle tips of MNs employing a dual-step molding method. The MN was pressed to the melanoma tumor site in mice, followed by exposure to an 808 nm laser for a duration of 4 min. The temperature at the treatment site rapidly reached 55 °C and remained constant during the exposure time. Findings from animal experiments indicated that tumors were almost completely eradicated without recurrence after 2 weeks in the MNs group, which was in stark contrast to the intratumor and intravenous injection groups. The full utilization of NIR950's photothermal energy can be achieved via the advantages of dissolving MNs without the need for systematic distribution. A solitary administration of a low dose, coupled with a single laser treatment, can achieve desirable antitumor effects, making the PTT of superficial tumors more accurate and controllable. In order to visualize the drug release process during PTT, the Poly-AM-TPE-CAA (PATC) was used to encapsulate the drug and photothermal agent, which changed the fluorescence intensity with temperature change. Li et al.^[206] created a self-monitoring pulse drug release system using a polymer MNs patch that underwent a visual phase change (Figure 6D). This technology allowed for real-time monitoring of drug release and enabled chemotherapeutic PTT synergistic treatment of melanoma. The researchers combined the chemotherapeutic drug DOX with the photothermal agent ICG within the PATC polymer to create particles called D/I@ PATC. These particles were then concentrated at the tip of the MNs to make patches known as D/I@ PATC-MN. This not only accomplished the visibility and confirmation of MN drug release, but also enhanced the photothermal stability and dependability in both in vitro and in vivo settings. In vitro investigations demonstrated that D/I@ PATC microparticles exhibit exceptional photo-controlled drug release capability and potent anti-tumor effects when administered in a low-dose single dose. Experiments conducted on living organisms revealed that a solitary administration of the D/I@ PATC-MN patch can effectively and precisely control chemical PTT for melanoma. This treatment substantially suppresses tumor growth without causing notable harm to the entire body, offering a novel approach to the clinical management of melanoma.

3.3. Stimulus-Responsive MNs-Mediated Chemotherapy

Chemotherapy is an effective means of systemic treatment for malignant tumors, but the traditional chemotherapeutic drugs are non-targeted, which will not only attack cancer cells, but also

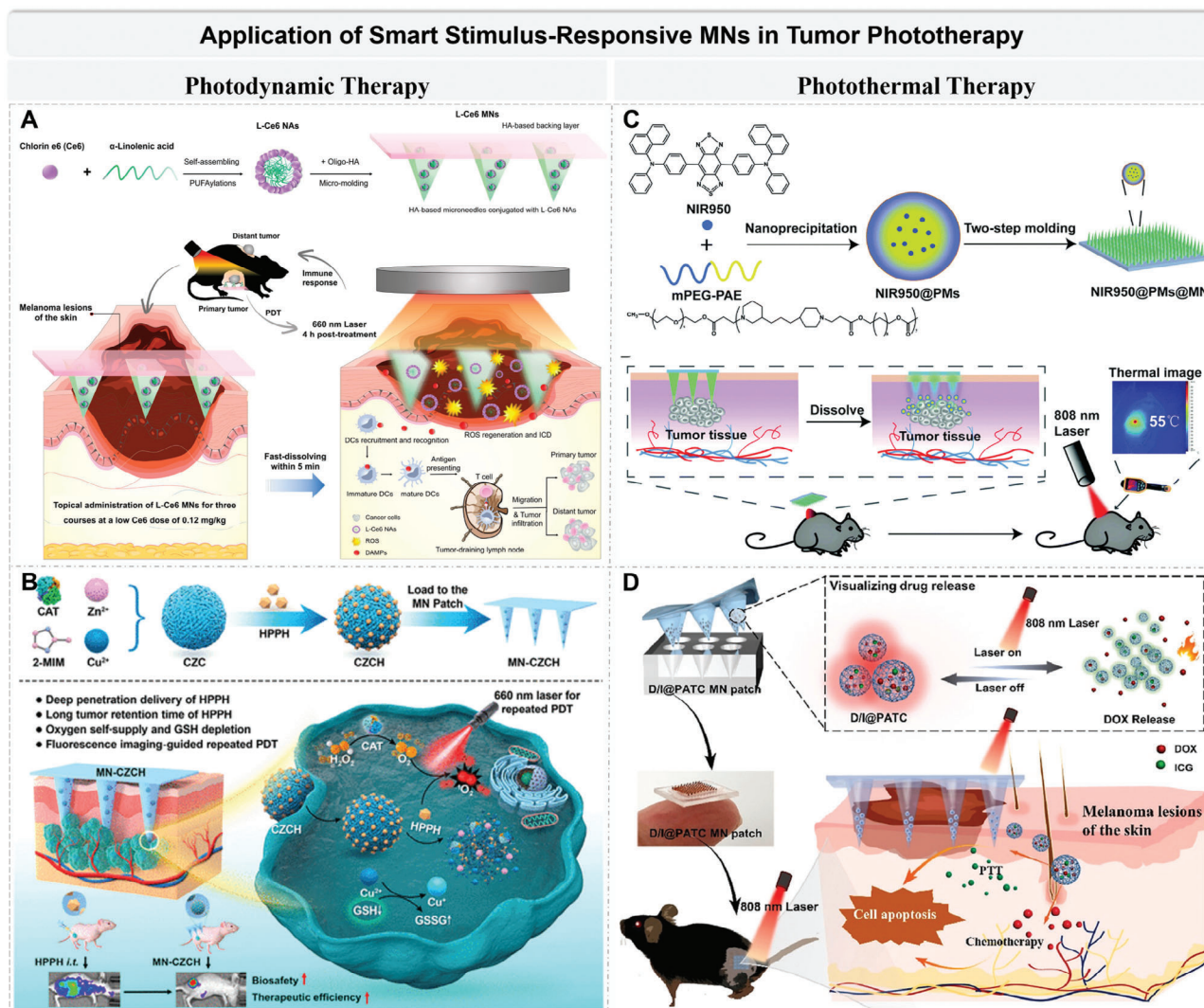


Figure 6. Stimulus-responsive MNs-mediated phototherapy. A) Schematic illustration of the facile fast-dissolving microneedles-based composite system with low-dose photosensitizers which enhanced antitumor immune response of photodynamic therapy. Reproduced with permission.^[54] Copyright 2021, American Chemical Society. B) Preparation Process of the CZCH and CZCH-Loaded MN Patch and Schematic Diagram of the MN-CZCH Patch for the Repeated PDT of Melanoma. Reproduced with permission.^[205] Copyright 2022, American Chemical Society. C) Schematic illustration of NIR950@PMs@MN application process and photothermal effect on B16 tumor-bearing C57 mice. Reproduced with permission.^[76] Copyright 2020, Royal Society of Chemistry. D) Schematic illustration of the D/I@PATC MN patch for melanoma therapy. Reproduced with permission.^[206] Copyright 2023, Elsevier.

cause damage to healthy cells, which often leads to a series of side effects, resulting in body damage and immune suppression. The development of highly precise local drug delivery methods is imperative for reducing the toxic effects associated with the systemic administration of chemotherapeutics, minimizing the impact on healthy cells while enhancing therapeutic efficacy. With the advancement of nanotechnology and biomaterials, new breakthroughs have been made in utilizing smart MNs for the localized delivery of chemotherapeutic drugs in the context of tumor treatment.

Lan et al. created pH-sensitive lipid-coated cisplatin NPs (LCC-NPs), which were embedded into dissolvable MNs using a molding technique (Figure 7A).^[129] These NPs can effectively regulate the release of cisplatin, significantly reduce non-specific toxicity,

increase cellular uptake, and enhance toxicity against tumor cells. Finally, the therapeutic impact on the head-and-neck cancers animal model was significantly improved, while general toxicity and adverse effects were kept to a minimum. These findings validate that MNs loaded with LCC-NPs serve as a secure and effective transdermal delivery method for chemotherapy, resulting in enhanced anticancer effects and reduced systemic toxicity. Besides, smart MNs combined with ultrasonic responsiveness can facilitate local delivery of chemotherapeutic drugs. Researchers have designed an electrochemical stimulator based on zinc oxide nanowires that can produce densely distributed MBs in the interstitial fluid of the tumor site.^[48] Then, driven by external ultrasound, local MBs were ruptured and tumor cells produced microcavitations, which had a great impact on the delivery effect of

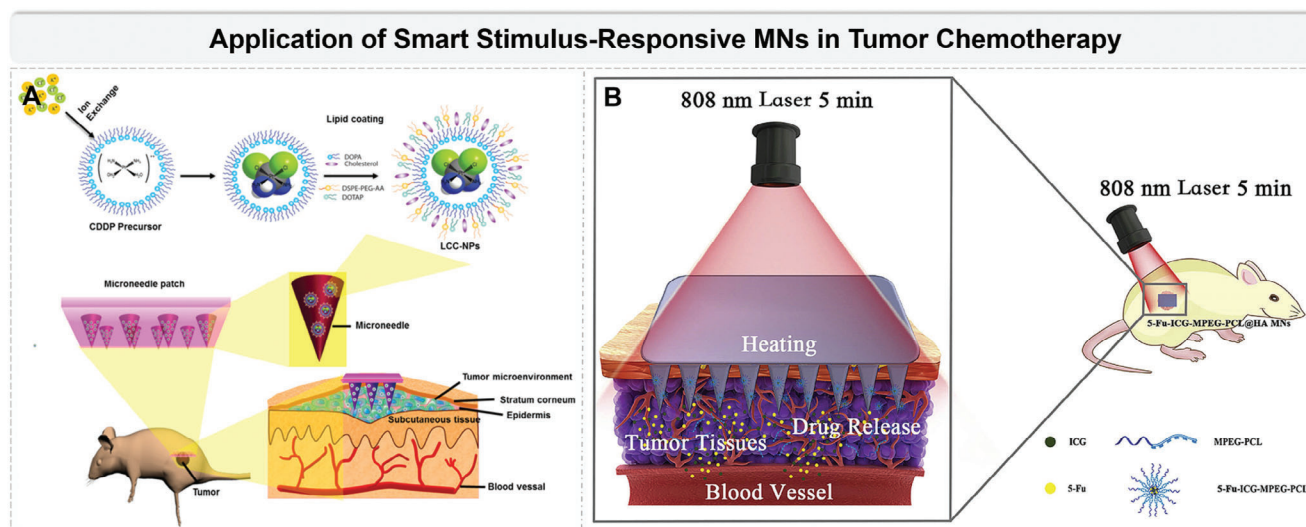


Figure 7. Stimulus-responsive MNs-mediated chemotherapy. A) Schematic illustration of a microneedle technique to mediate the transdermal delivery of lipid-coated cisplatin nanoparticles (LCC-NPs) for cancer therapy. Reproduced with permission.^[129] Copyright 2018, American Chemical Society. B) The schematic illustration of the skin cancer treatment by 5-Fu-ICG-MPEG-PCL@HA MN under 808 nm laser within 5 min. Reproduced with permission.^[68] Copyright 2020, Elsevier.

antitumor drugs. In vivo experiments showed a more than five-fold decrease in tumor dimensions following a 10-day period of ultrasound-assisted chemotherapy compared with chemotherapy alone. In addition, the method enabled them to reduce the PTX dosage to 25% effective dosage. This treatment approach may provide a promising strategy to reduce the side effects via tumor-targeted therapy.

Qian et al.^[68] created an MNs system that combined drugs and NPs to treat squamous cell carcinoma and melanoma (Figure 7B). The technology used NIR light to activate the drugs and deliver them through the skin. This research involved the combination of polyethylene glycol PCL NPs, which contained both 5-Fu and ICG, with HA-soluble MNs using the template approach. These MNs enhanced the efficiency of delivering drugs via the skin, enabled the targeted administration of drugs to tumors through the skin, and mitigated the adverse effects of drugs on the body. Moreover, the insertion of MNs into tumor tissue resulted in the release of drug-loaded NPs as the MNs dissolved. Upon exposure to 808 nm NIR light, the ICG included in the NPs underwent a process of converting light energy into thermal energy. By applying both chemotherapy and PTT, the NPs effectively heated the tumor tissue and eliminated tumor cells. Additionally, they regulated the release of 5-Fu, attaining the desired outcome of synergistic treatment for skin cancer. This was a hybrid system capable of administering chemotherapeutic medications with PTT performance.

In addition to the above two drugs, chemotherapy drugs that are often used in combination with stimulus-responsive MNs include PTX^[207] and DOX^[57,59,69,72] for anti-tumor therapy.

3.4. Stimulus-Responsive MNs-Mediated Gene Therapy

Gene therapy is an alternative treatment that introduces specific genetic material (DNA, RNA, mRNA, siRNA, etc.) into cancer

cells or tissues to alter the expression of genes or regulate the biological characteristics of the tissue, causing cell death or slowing the growth of cancer.^[208] Recently, new breakthroughs have also been made in the use of smart MNs to deliver genes for tumor treatment. The p53 expression plasmid (p53 DNA) is a type of tumor cell suppressor gene and has been utilized in numerous studies to hinder the growth of tumors.^[209] Li et al.^[128] used LBL assembly technology to prepare pH-sensitive MNs covered with PEM, rapidly releasing genes to achieve subdermal tumor treatment (Figure 8A). The PEM consisted of the pH-sensitive transition layers (PLL-DMA/polyethyleneimine)₁₂ and the gene-loaded layers (p53 DNA/polyethyleneimine)₁₆. Under simulated cutaneous conditions with a pH of 5.5, MNs containing both drug-loaded layers and transition layers (marked as tr-MNP) were able to release 33% of DNA, while MNs without transition layers (marked as ntr-MNP) only managed to release 4%. The tumor inhibition effect of tr-MNP on subcutaneous tumor-bearing mice was substantially higher than that of the impact of ntr-MNP and intravenous groups.

Zhang et al.^[210] created soluble MNs (IR780-PL) embedded with NPs that possessed controllable and reflective characteristics (Figure 8B). In order to accomplish precise delivery of FBXO₄₄, which targeted the CRISPR/Cas9 plasmid (pFBXO₄₄), along with a hydrophobic PS. Biocompatible oligo-HA were used to create dissolved MNs (DMNs) that can adapt to the uneven shape of superficial tumor lesions. Subsequently, researchers incorporated NPs into DMNs (IR780-PL/pFBXO₄₄@MN). Prior to applying the IR780-PL/pFBXO₄₄@MN, collagenase MNs underwent a pretreatment process to break down the tumor matrix and enhance the ability of IR780-PL/pFBXO₄₄ NPs to penetrate the inner layers of the tumor. When exposed to 880 nm light, IR780-PL/pFBXO₄₄ NPs generated ROS for PDT. Simultaneously, photochemical internalization enhanced the process of lysosomal escape, resulting in the liberation of the pFBXO₄₄ plasmid by breaking the disulfide bond of NPs within the cytoplasm.

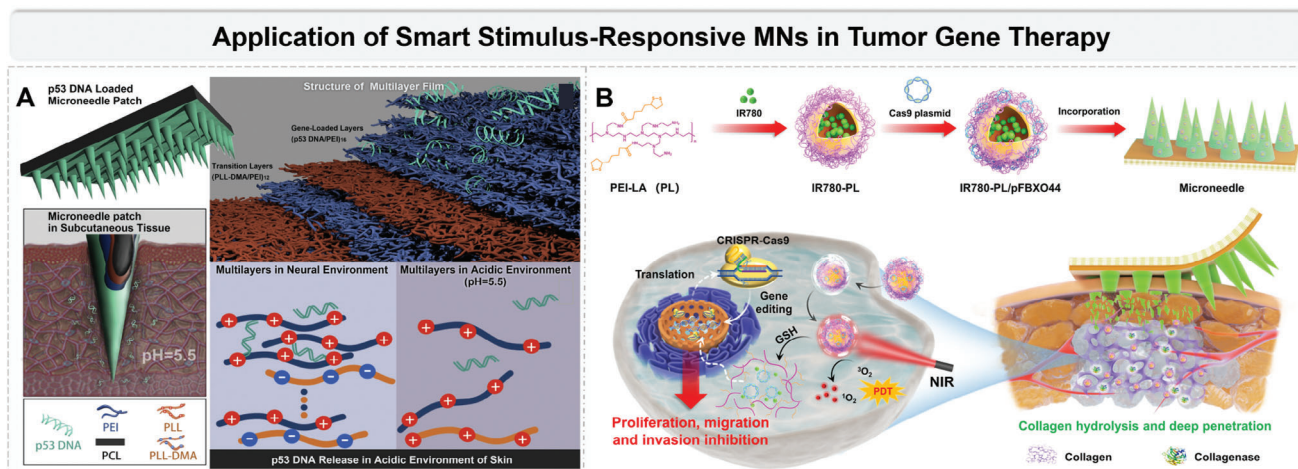


Figure 8. Stimulus-responsive MNs-mediated gene therapy. A) The scheme of the microneedle patch is modified with pH-responsive transition layers and gene-loaded layers by layer-by-layer assembly. Reproduced with permission.^[128] Copyright 2019, Elsevier. B) Schematic illustration of NPs-embedded dissolving microneedles for antitumor therapy. Reproduced with permission.^[210] Copyright 2023, American Chemical Society.

Hence, IR780-PL/pFBXO₄₄ exhibited proficient disruption of FBXO₄₄ at the genomic level in cancer cells, while also possessing the ability to modulate its spatial and temporal aspects. This technique resulted in a synergistic impact by combining gene therapy and phototherapy, leading to the effective eradication of malignancies. The in vivo anticancer impact was investigated using a 4T1 mouse model. Comparing with the control group, it was found that IR780-PL@MNs + L and PL/pFBXO₄₄@MNs effectively suppress tumor growth. In comparison to the single treatment group, the IR780-PL/pFBXO₄₄@MNs + L group exhibited differences. The coadministration of IR780 with gene therapy in the IR780-PL/pFBXO₄₄@MNs + L group exhibited a heightened anticancer efficacy and a diminished rate of tumor regrowth.

3.5. Stimulus-Responsive MNs-Mediated Targeted Therapy

Targeted therapy is an approach to treatment that focuses on particular molecules or signaling pathways within tumor cells, allowing for a more precise attack on tumor cells and minimizing harm to healthy cells. These treatments, based on molecular and genetic differences between tumor cells and normal cells, inhibit tumor development by interfering with tumor cell survival, proliferation, growth, or signaling. Clinically, targeted therapeutic drugs are often administered orally in high dosages, insulating in limited bioavailability, and a spectrum of side effects that could pose life-threatening risks.^[211] Therefore, local targeted drug delivery using stimulus-responsive MNs as nanocarriers can enhance the concentration of specific drugs at the region of the tumor, thereby considerably alleviating the systemic load on the body.

The distinguishing characteristic of melanoma is the dysregulation of mitogen-activated protein kinase (MAPK) signaling, and ≈50% of patients with metastatic skin melanoma exhibit mutations within the *BRAF* gene.^[212] Notably, melanoma cells carrying the BRAFV600 mutation are dependent on the RAF/MEK/ERK signaling pathway.^[213] Due to the enhancements in overall survival as validated in multiple international cen-

ters randomized trials, two small molecule inhibitors targeting *BRAF*, namely dabrafenib, and vemurafenib, in addition to an MEK inhibitor called trametinib, have gained approval for the management of metastatic melanoma with *BRAF* mutation. On this basis, Tham et al.^[75] designed a photodynamically active MNs carrier loaded with targeted therapeutic drugs (Figure 9A). Mesoporous organo-silica NPs incorporated into MNs, carrying trametinib and dabrafenib, are designed to specifically target the overactive MAPK pathway for the treatment of melanoma. The drug-loaded nanocarriers exhibit a synergistic lethal effect on tumor cells under NIR irradiation, while retaining their non-toxicity toward non-BRAF mutant cells. Experiments on tumor regression conducted in xenografted murine models have verified the enhanced therapeutic effectiveness of nanocarriers achieved by combining PDT with targeted therapy.

In order to overcome drug resistance, the proteolysis targeting chimera (PROTAC) concept was developed. Cheng et al.^[214] combined the ERD308 and Palbociclib (FDA approved CDK4/6 inhibitor) with in pH-sensitive MPEG-poly(β -amino ester) (MPEG-PAE) micelles (Figure 9B). These micelles were then placed into HA-based MNs patches to create a drug delivery system that targeted the ER α . To assess the pH responsiveness of MPEG-PAE micelles and determine if drug release triggered by pH led to increased cellular uptake, the researchers performed a set of experiments. Tissue slice fluorescence imaging results demonstrated that pH-sensitive micelles, in comparison to the non-pH-sensitive group, exhibited a 48.6-fold increase in drug delivery to the tumor location, while concurrently reducing drug delivery to the liver by 40%. It was discovered that MNs patches had more precise control over medication distribution compared to intravenous administration. The drug signals were localized specifically in the tumor tissue area. The biodistribution data indicated that MNs patches filled with micelles can effectively transport more than 87% of medicines to tumor tissue and achieve significant penetration into the tumor. Oral PROTACs, which need to be taken daily, are less effective than single-dose PROTAC-loaded MNs patches, which can maintain their effectiveness for a minimum of 4 days. The simultaneous injection of ERD308 and Pal-

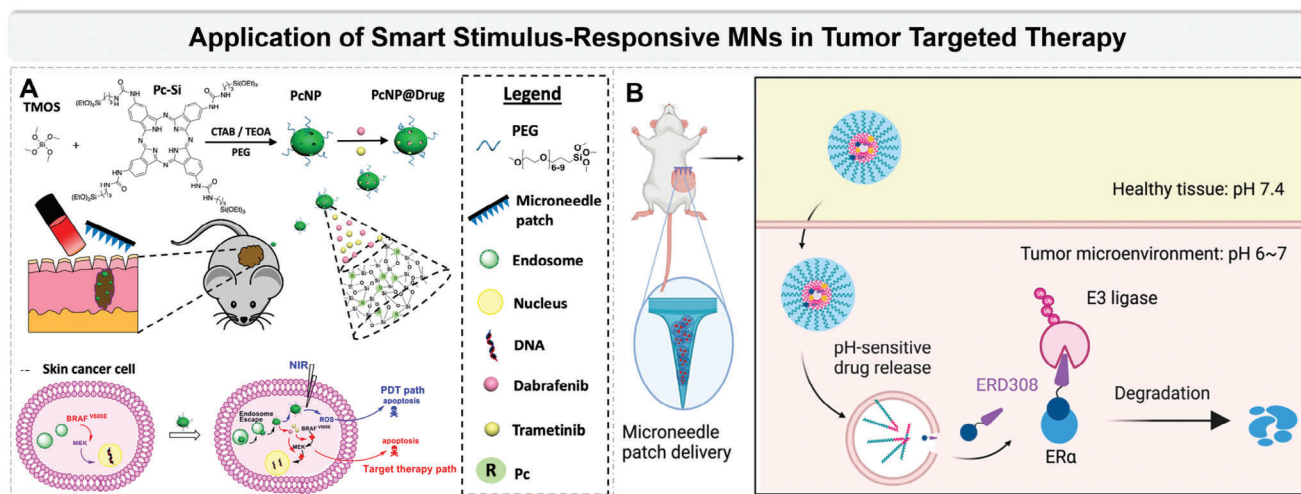


Figure 9. Stimulus-responsive MNs-mediated targeted therapy. A) Synthesis, penetration into diseased skin, and cellular mechanism of PcNP@Drug. Reproduced with permission.^[75] Copyright 2018, American Chemical Society. B) The scheme of a pH-sensitive micelle loading into microneedle patch delivery of PROTACs for anti-cancer therapy. Reproduced with permission.^[214] Copyright 2023, American Chemical Society.

bociclib resulted in a tumor therapy rate of over 80% in mouse tumor models that were positive for ER. Safety experimental results showed the absence of inflammation or skin irritation at the site of administration, as well as the absence of any histological alterations in the major organs. Additionally, the study revealed that MNs had no impact on blood glucose levels, liver function, and kidney function in mice, indicating that the medication delivery mechanism did not cause any negative effects on the body.

3.6. Stimulus-Responsive MNs-Mediated Multimodal Synergy Therapy

A single treatment has limitations, which might result in ineffective treatment, medication resistance, side effects, metastasis, and cancer recurrence. As a result, multimodal synergy therapy is an excellent technique for treating tumors.

Recently, MN-based PDT and PTT combined with chemotherapy, immunotherapy, and targeted therapy have made great progress in the synergistic treatment strategies for tumors. NIR-responsive PEGylated gold nanorod (GNR-PEG) coated with poly (L-Lactide) MNs (GNR-PEG@MNs) have been prepared to increase the anti-tumor efficiency of micelles (Figure 10A).^[70] GNR-PEG@MNs had good thermal transmission capabilities in the body, achieving a temperature of 50 °C at the region of the tumor within a mere 5-min timeframe. Compared with simple chemotherapy and PTT, the combination therapy involving GNR-PEG@MNs and low-dose MPEG-PDLLA-DTX micelles (at 5 mg kg⁻¹) had the capability to achieve a complete cure of tumors, with no subsequent recrudescence in the body. This combined approach exhibited significant synergistic effects. More attractively, Wang et al.^[61] designed multifunctional SF MNs, incorporating a targeted drug (bevacizumab) along with chemotherapeutic agents (thrombin and temozolomide) (Figure 10B). By adjusting the time of ethanol annealing, altering the level of crosslinking, and employing transcranial NIR light irradiation as an activa-

tor, it is possible to achieve controlled, staged release of the trio of drugs at a specific time and space. This approach can effectively contribute to apoptosis of glioblastoma cells, anti-angiogenesis, and hemostasis.

Ye et al.^[79] devised a melanin-amplified cancer immunotherapy method utilizing transdermal MNs patches (Figure 10C). They loaded the lysate of melanoma cells into a MNs array. When topically applied to the skin, which was the greatest immunological organ in the human body, melanin MNs stimulated an immune response, leading to a quicker immune system reaction to melanoma cells and enhancing the efficacy of the response. By exposing therapeutic patches to NIR light, the heat generated locally induced a fever-like condition in the skin, which enhanced the release of lysates from MNs and successfully attracted and activated immune cells. The heightened temperature additionally facilitated the localized augmentation of blood and lymphatic circulation, hence fostering the movement of immune cells. This enhanced immune response improved the body's capacity to recognize and react to lysates, more effectively inhibiting the development of melanoma.

Besides, Zhao et al.^[215] conducted a study on MN-mediated treatment of melanoma by utilizing the ferroptosis pathway (Figure 10D). They employed porous silicon (PSi) loaded with dual nanozymes, which were integrated with MNs patches. Nanozymes can effectively infiltrate the dermis, where melanoma is situated, by utilizing reversible microchannels formed inside MNs. The combined catalytic characteristics of several nanozymes were anticipated to counteract the adverse effects of the complex TME, hence delivering effective and uncomplicated treatment of tumors. This offered a promising approach to the clinical management of melanoma. In a B16-F10 tumor nude mice model, the external photothermal effect caused by NIR radiation can greatly enhance the catalytic efficiency of nanozymes. The findings demonstrated that, during a 14-day treatment period, only the group of nude mice subjected to NIR stimulation exhibited uncontrolled tumor growth. The combination of HA MNs and NIR stimulation effectively

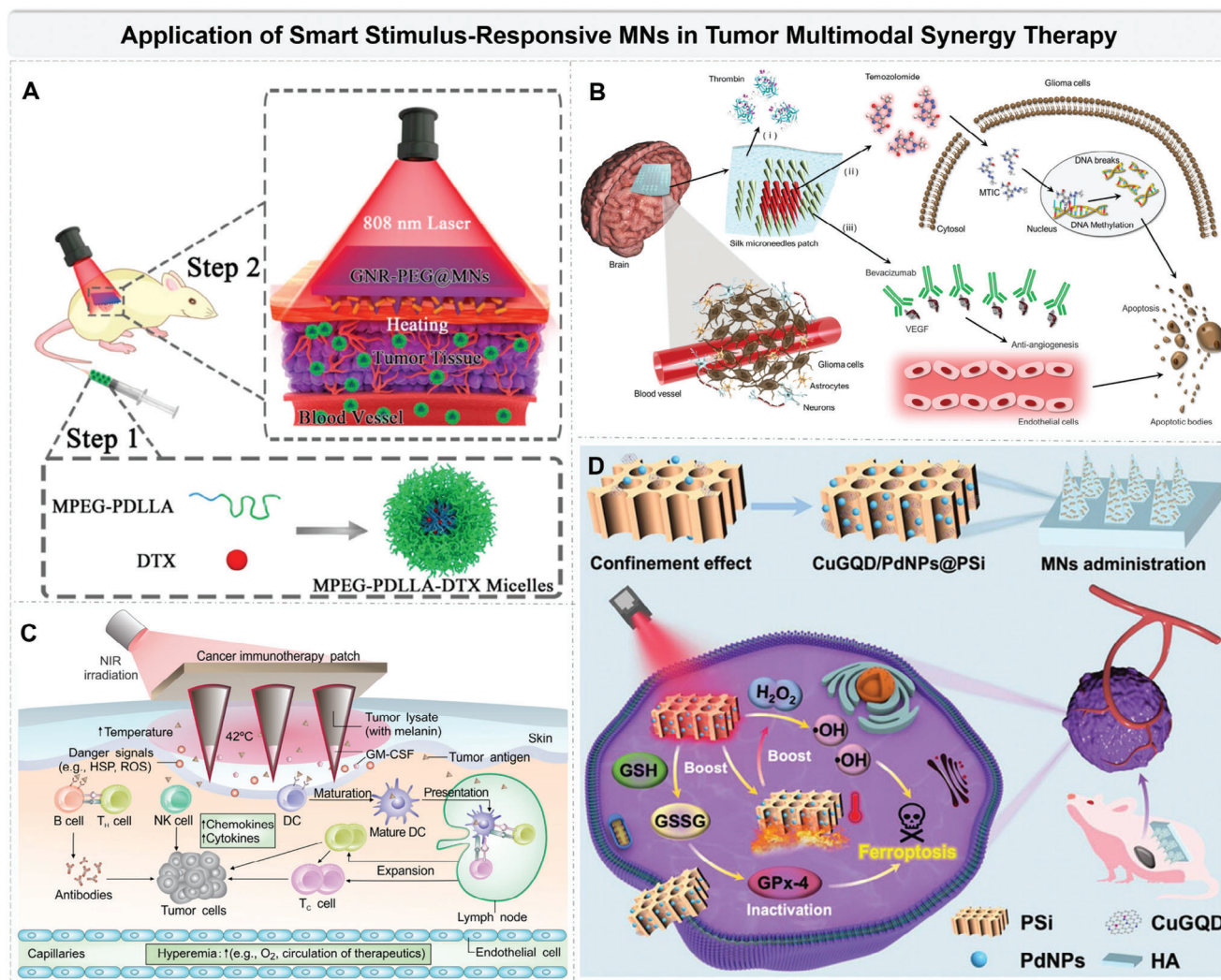


Figure 10. Stimulus-responsive MNs-mediated multimodal synergistic therapy. A) The novel synergistic system of chemotherapy and photothermal therapy to treat A431 tumors by the combination of near-infrared responsive GNR-PEG@MNs and MPEG-PDLLA-DTX micelles. Reproduced with permission.^[70] Copyright 2017, American Chemical Society. B) Schematic of multidrug-integrated silk fibroin microneedle patches for in situ treatment of glioblastoma. Reproduced with permission.^[61] Copyright 2022, WILEY. C) Schematic illustration of MN-based transdermal vaccination. Reproduced with permission.^[79] Copyright 2017, AAAS. D) Schematic illustration of microneedle integrated with PSi loaded with bifunctional nanozymes to induce ferroptosis of subcutaneous melanoma through nanocatalytic strategy. Reproduced with permission.^[215] Copyright 2020, WILEY.

suppressed tumor development. Partial inhibition of tumor growth can be achieved by modulating the levels of endogenous H_2O_2 and GSH. In vivo, the augmented peroxidase response of PTT can effectively hinder the progression of melanoma. And, the majority of tumors in the MNs + NIR group experienced a significant reduction or total regression within 2 weeks, exhibiting a Tumor Growth Inhibition value of up to 98.8%. The MNs + NIR group exhibited the most potent cytotoxicity against cancer cells and effectively suppressed their proliferation. This was attributed to the significant downregulation of GPx-4, suggesting that the reduced expression of GPx-4 triggers ferroptosis, leading to anti-tumor actions. The aforementioned findings revealed that the synergistic therapy of multi-nanozyme therapy combined with MNs can effectively treat melanoma through the ferroptosis pathway.

4. Current Challenges and Outlook

Recently, as a local drug delivery system, MNs patch has become a popular research direction in anti-tumor therapy. Researchers have combined the characteristics and advantages of MNs with clinical needs to develop functional MNs with good biocompatibility, intelligent responsiveness, and multi-mode collaborative therapy. Through the design of matrix materials, researchers have endowed smart MNs with various physical and chemical properties to adapt to specific tumor microenvironments and realized the anti-tumor purpose of combining chemotherapy, immunological therapy, gene therapy, targeted therapy, phototherapy, and other approaches through the combination of different types of encapsulated therapeutic agents. In particular, multimodal collaborative anti-tumor smart MNs can not only achieve

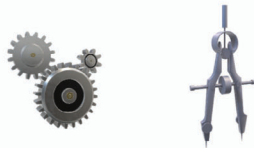

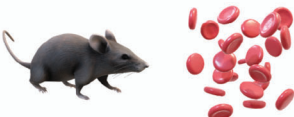
Outlook of Stimulus-responsive MNs in Antitumor Therapy		
Level	Challenges	Measures
Technology & Technique 	<ul style="list-style-type: none"> • Complex manufacturing process, • Difficult to mass produce • Limited drug load • Sensitivity and specificity to be improved 	<ul style="list-style-type: none"> • Material design and innovation • Technics iteration and upgrading
Quality Control & Cost 	<ul style="list-style-type: none"> • High investment in sterile conditions • Lack of industry quality control standards and management criteria • Difficult to ensure the product consistency • Biosafety remains a key concern 	<ul style="list-style-type: none"> • Simplified design • Uniform guidelines and consensus • Optimize biocompatibility
Study Design & Validation 	<ul style="list-style-type: none"> • Tissue differences between rodents and humans • Lack of high-quality <i>in vivo</i> pharmacokinetics and pharmacodynamics evaluation 	<ul style="list-style-type: none"> • Parameter optimization based on human body structure • To improve the metabolism study <i>in vivo</i>

Figure 11. Future prospects of stimulus-responsive MNs in antitumor therapy.

local drug delivery and target tumor tissues, but also reduce the amount of anti-tumor drugs, systemic toxicity, and drug resistance. At the same time, this kind of drug delivery platform can activate the systemic immune system and achieve systemic antimetastasis, which may be an important trend for future research.

Although stimulus-responsive MNs are particularly appealing for tumor treatment, they have rarely been commercialized or entered into the stage of clinical trials. Among them, there are several reasons that hinder the clinical transformation of smart MNs for cancer treatment: 1) the production procedure for stimulus-responsive MNs is complex and incurs high costs, so there are great challenges for bulk production and quality control; 2) due to lack of specific quality control standards and management criteria in the industry, the product consistency and biosafety is still a major problem; 3) lack of high-quality *in vivo* pharmacokinetics and pharmacodynamics evaluation experiments; 4) the preparation and production process of smart MNs need strict aseptic conditions, and the investment in disinfection and sterilization technology and aseptic workshop is relatively high; 5) the drug loading of MNs isn't sufficient for sustained treatment; 6) the sensibility and specificity of smart MNs to stimulus signals need to be improved. In short, the design of stimulus-responsive MNs should be based on easy clinical transformation, rather than blindly pursuing complex structures or emerging methods.

What is noticeable is that preclinical studies of stimulus-responsive MNs have overwhelmingly focused on rodents. Compared with mouse skin, human skin exhibits a thicker epidermis and dermis, along with less densely packed hair follicles. In future transformation studies, it is imperative to further refine the size, morphology, and mechanical characteristics of the MNs arrays, taking into consideration the practicality for human applications. Obviously, there is a significant imbalance in the research development of responsive MNs based on different stimuli. Researchers are often limited by the characteristics of the tumor microenvironment to design smart MNs, so that some types of responsive MNs are rarely studied (e.g., magnetic response, mechanical response, etc.). In view of the above problems, researchers need to consider the sustainable development of smart MNs from many aspects in the near future, including availability and stability of smart materials, soft and painless wearability, diversity, accuracy and sensitivity of responsive mode, excellent biocompatibility and safety, technics iteration and upgrading, feasibility and economy of easy mass production, uniform guidelines and consensus and so on. **Figure 11** shows future prospects of stimulus-responsive MNs in antitumor therapy, which is discussed from the prospects of stimulus-responsive MNs at the technology, process, quality control, cost, study design, and validation levels, respectively.

5. Conclusion

In summary, the rapid advancement in biological functional materials and manufacturing techniques opens up boundless opportunities for the growth of stimulus-responsive MNs systems. Under biochemical (enzyme, glucose, pH, oxygen, etc.) or physical (ultrasound, light, electricity, temperature, force, magnetic field, etc.) stimulation, these smart MNs undergo a series of changes, such as the release of cargo caused by the phase transformation of MNs, thermal ablation and oxidative stress reaction of local action site, and finally achieve the purpose of treatment. As a user-centered intelligent carrier that takes the actual changes of the disease condition as the trigger signal to play the therapeutic effect, it is a unique “closed-loop” treatment mode, which makes the treatment effect more accurate and controllable. Compared with ordinary MNs, smart responsive MNs can reduce local or systemic complications caused by overtreatment or overmedication. Overall, a smart MNs system has the advantages of being tiny and lightweight, soft and wearable, painless and minimally invasive, safe and efficient, on-demand and controllable, and economic and environmental protection. Although the clinical transformation of smart MNs is facing difficulties and obstacles, smart MNs have a broad application prospect and considerable market value.

Acknowledgements

H.C. and J.X. contributed equally to this work. This research was funded by the National Key Research and Development Program of China (2022YFE0111700, 2022YFB3804703, and 2022YFB3205602), the National Natural Science Foundation of China (T2125003, 61875015, and 52372174), the Beijing Natural Science Foundation (L212010, L212046 and JQ20038), along with the Fundamental Research Funds for the Central Universities (E0EG6802x2).

Conflict of Interest

The authors declare no conflict of interest.

Keywords

cancer therapy, drug-controlled release, microneedles, stimulus-responsive

Received: October 21, 2023
Revised: December 9, 2023
Published online:

- [1] K. D. Miller, M. Fidler-Benaoudia, T. H. Keegan, H. S. Hipp, A. Jemal, R. L. Siegel, *Ca-Cancer J. Clin.* **2020**, *70*, 443.
- [2] Y. Yang, W. Zeng, P. Huang, X. Zeng, L. Mei, *View* **2021**, *2*, 20200042.
- [3] M. Arruebo, N. Vilaboa, B. Sáez-Gutiérrez, J. Lambea, A. Tres, M. Valladares, Á. González-Fernández, *Cancers* **2011**, *3*, 3279.
- [4] C. Tang, M. J. Livingston, R. Safirstein, Z. Dong, *Nat. Rev. Nephrol.* **2023**, *19*, 53.
- [5] M. J. O'Connor, *Mol. Cell* **2015**, *60*, 547.
- [6] Z. Yang, H. Chen, *View* **2022**, *3*, 20220009.
- [7] Y. Li, Q. Bao, S. Yang, M. Yang, C. Mao, *View* **2022**, *3*, 20200027.
- [8] C. o. Drugs, *Pediatrics* **1997**, *100*, 143.
- [9] C. Pegoraro, S. Macneil, G. Battaglia, *Nanoscale* **2012**, *4*, 1881.
- [10] S. M. Pond, T. N. Tozer, *Clin. Pharmacokinet.* **1984**, *9*, 1.
- [11] I. Usach, R. Martinez, T. Festini, J.-E. Peris, *Adv. Ther.* **2019**, *36*, 2986.
- [12] T. Waghule, G. Singhvi, S. K. Dubey, M. M. Pandey, G. Gupta, M. Singh, K. Dua, *Biomed. Pharmacother.* **2019**, *109*, 1249.
- [13] Y. Zhang, Y. Xu, H. Kong, J. Zhang, H. F. Chan, J. Wang, D. Shao, Y. Tao, M. Li, *Exploration* **2023**, *3*, 20210170.
- [14] X. Jiang, W. Zhang, R. Terry, W. Li, *BMEMat* **2023**, *1*, e12044.
- [15] Y.-C. Kim, J.-H. Park, M. R. Prausnitz, *Adv. Drug Delivery Rev.* **2012**, *64*, 1547.
- [16] A. S. Rzhvskiy, T. R. R. Singh, R. F. Donnelly, Y. G. Anissimov, *J. Control Release* **2018**, *270*, 184.
- [17] S. Kaushik, A. H. Hord, D. D. Denson, D. V. McAllister, S. Smitra, M. G. Allen, M. R. Prausnitz, *Anesth. Analg.* **2001**, *92*, 502.
- [18] S. Indermun, R. Luttge, Y. E. Choonara, P. Kumar, L. C. Du Toit, G. Modi, V. Pillay, *J. Control Release* **2014**, *185*, 130.
- [19] H. L. Quinn, M.-C. Kearney, A. J. Courtenay, M. T. McCrudden, R. F. Donnelly, *Expert Opin. Drug Delivery* **2014**, *11*, 1769.
- [20] L. Wei-Ze, H. Mei-Rong, Z. Jian-Ping, Z. Yong-Qiang, H. Bao-Hua, L. Ting, Z. Yong, *Int. J. Pharm.* **2010**, *389*, 122.
- [21] S. P. Davis, W. Martanto, M. G. Allen, M. R. Prausnitz, *IEEE Trans. Biomed. Eng.* **2005**, *52*, 909.
- [22] M. A. Boks, W. W. J. Unger, S. Engels, M. Ambrosini, Y. V. Kooyk, R. Luttge, *Int. J. Pharm.* **2015**, *491*, 375.
- [23] A. M. De Groot, A. C. M. Platteel, N. Kuijt, P. J. S. Van Kooten, P. J. Vos, A. J. A. M. Sijts, K. Van Der Maaden, *Front. Immunol.* **2017**, *8*, 1789.
- [24] C. J. Martin, C. J. Allender, K. R. Brain, A. Morrissey, J. C. Birchall, *J. Control Release* **2012**, *158*, 93.
- [25] P. N. Ayittey, J. S. Walker, J. J. Rice, P. P. De Tombe, *Pflügers Archiv-Eur. J. Physiol.* **2009**, *457*, 1415.
- [26] X. Jin, D. D. Zhu, B. Z. Chen, M. Ashfaq, X. D. Guo, *Adv. Drug Delivery Rev.* **2018**, *127*, 119.
- [27] J. G. Turner, L. R. White, P. Estrela, H. S. Leese, *Macromol. Biosci.* **2021**, *21*, 2000307.
- [28] J. Yu, Y. Zhang, A. R. Kahkoska, Z. Gu, *Curr. Opin. Biotechnol.* **2017**, *48*, 28.
- [29] Y. Lu, A. A. Aimetti, R. Langer, Z. Gu, *Nat. Rev. Mater.* **2016**, *2*, 16075.
- [30] A. Geraili, M. Xing, K. Mequanint, *View* **2021**, *2*, 20200126.
- [31] X. Zhang, Y. Wang, J. Chi, Y. Zhao, *Research* **2020**, <https://doi.org/10.34133/2020/7462915>.
- [32] P. Singh, A. Carrier, Y. Chen, S. Lin, J. Wang, S. Cui, Xu Zhang, *J. Control Release* **2019**, *315*, 97.
- [33] D. Berillo, Z. Zharkinkbekov, Y. Kim, K. Raziyeve, K. Temirkhanova, A. Saparov, *Pharmaceutics* **2021**, *13*, 2050.
- [34] S. Mura, J. Nicolas, P. Couvreur, *Nat. Mater.* **2013**, *12*, 991.
- [35] E. M. Cahill, E. D. O'carbhaill, *Bioconjugate Chem.* **2015**, *26*, 1289.
- [36] Y. Yang, R. Luo, S. Chao, J. Xue, D. Jiang, Y. H. Feng, X. D. Guo, D. Luo, J. Zhang, Z. Li, Z. L. Wang, *Nat. Commun.* **2022**, *13*, 6908.
- [37] B. H. J. Gowda, M. G. Ahmed, A. Sahebkar, Y. Riadi, R. Shukla, P. Kesharwani, *Biomacromolecules* **2022**, *23*, 1519.
- [38] Y. Lu, W. Sun, Z. Gu, *J. Control Release* **2014**, *194*, 1.
- [39] D. Zhi, T. Yang, J. O'hagan, S. Zhang, R. F. Donnelly, *J. Control Release* **2020**, *325*, 52.
- [40] Y. Tao, H. F. Chan, B. Shi, M. Li, K. W. Leong, *Adv. Funct. Mater.* **2020**, *30*, 2005029.
- [41] Y. Zhao, Z. Zhang, Z. Pan, Y. Liu, *Exploration* **2021**, *1*, 20210089.
- [42] Y. Liu, M. Sun, T. Wang, X. Chen, H. Wang, *View* **2021**, *2*, 20200069.
- [43] P. Makvandi, R. Jamaledin, G. Chen, Z. Baghbantargarhdari, E. N. Zare, C. Di Natale, V. Onesto, R. Vecchione, J. Lee, F. R. Tay, P. Netti, V. Mattoli, A. Jaklenec, Z. Gu, R. Langer, *Mater. Today* **2021**, *47*, 206.
- [44] M. A. Wheatley, M. Cochran, *J. Drug Delivery Sci. Technol.* **2013**, *23*, 57.

- [45] L. Tu, Z. Liao, Z. Luo, Y. L. Wu, A. Herrmann, S. Huo, *Exploration* **2021**, 1, 20210023.
- [46] K. W. Ferrara, *Adv. Drug Delivery Rev.* **2008**, 60, 1097.
- [47] K. S. Suslick, N. C. Eddingsaas, D. J. Flannigan, S. D. Hopkins, H. Xu, *Acc. Chem. Res.* **2018**, 51, 2169.
- [48] A. Zandi, M. A. Khayamian, M. Saghaei, S. Shalileh, P. Katebi, S. Assadi, A. Gilani, M. Saleemizadeh Parizi, S. Vanaei, M. R. Esmailnejad, F. Abbasvandi, P. Hoseinpour, M. Abdolhad, *Adv. Healthcare Mater.* **2019**, 8, 1900613.
- [49] S. Shao, S. Wang, L. Ren, J. Wang, X. Chen, H. Pi, Y. Sun, C. Dong, L. Weng, Y. Gao, L. Wang, *ACS Appl. Bio Mater.* **2022**, 5, 562.
- [50] M. Bok, Z.-J. Zhao, S. Jeon, J.-H. Jeong, E. Lim, *Sci. Rep.* **2020**, 10, 2027.
- [51] J. G. Hardy, E. Larrañeta, R. F. Donnelly, N. Mcgoldrick, K. Migalska, M. T. C. McCrudden, N. J. Irwin, L. Donnelly, C. P. McCoy, *Mol. Pharmaceutics* **2016**, 13, 907.
- [52] Z. Zheng, H. Ye, J. Wang, T. Zhang, Q. You, H. Li, R. He, Y. Chen, W. Zhang, Y. Cao, *J. Mater. Chem. B* **2017**, 5, 7014.
- [53] S. Zhang, Z. Zhou, J. Zhong, Z. Shi, Y. Mao, T. H. Tao, *Adv. Sci.* **2020**, 7, 1903802.
- [54] Q. Bian, L. Huang, Y. Xu, R. Wang, Y. Gu, A. Yuan, X. Ma, J. Hu, Y. Rao, D. Xu, H. Wang, J. Gao, *ACS Nano* **2021**, 15, 19468.
- [55] S. Luo, Y. Zhao, K. Pan, Y. Zhou, G. Quan, X. Wen, X. Pan, C. Wu, *Biomater. Sci.* **2021**, 9, 6772.
- [56] P. Liu, Y. Fu, F. Wei, T. Ma, J. Ren, Z. Xie, S. Wang, J. Zhu, L. Zhang, J. Tao, J. Zhu, *Adv. Sci.* **2022**, 9, 2202591.
- [57] M.-C. Chen, Z.-W. Lin, M.-H. Ling, *ACS Nano* **2016**, 10, 93.
- [58] M.-C. Chen, M.-H. Ling, K.-W. Wang, Z.-W. Lin, B.-H. Lai, D.-H. Chen, *Biomacromolecules* **2015**, 16, 1598.
- [59] M.-C. Chen, K.-W. Wang, D.-H. Chen, M.-H. Ling, C.-Y. Liu, *Acta Biomater.* **2015**, 13, 344.
- [60] Y. Li, X. Liao, B. Zheng, *J. Biomater. Sci., Polym. Ed.* **2022**, 33, 155.
- [61] Z. Wang, Z. Yang, J. Jiang, Z. Shi, Y. Mao, N. Qin, T. H. Tao, *Adv. Mater.* **2022**, 34, 2106606.
- [62] Y. Zhao, Y. Zhou, D. Yang, X. Gao, T. Wen, J. Fu, X. Wen, G. Quan, X. Pan, C. Wu, *Acta Biomater.* **2021**, 135, 164.
- [63] M. Chen, G. Quan, T. Wen, P. Yang, W. Qin, H. Mai, Y. Sun, C. Lu, X. Pan, C. Wu, *ACS Appl. Mater. Interfaces* **2020**, 12, 32259.
- [64] J. Cui, J. Huang, Y. Yan, W. Chen, J. Wen, X. Wu, J. Liu, H. Liu, C. Huang, *J. Colloid Interface Sci.* **2022**, 617, 718.
- [65] L. Dong, Y. Li, Z. Li, N. Xu, P. Liu, H. Du, Y. Zhang, Y. Huang, J. Zhu, G. Ren, *ACS Appl. Mater. Interfaces* **2018**, 10, 9247.
- [66] L. Fan, X. Zhang, X. Liu, B. Sun, L. Li, Y. Zhao, *Adv. Healthcare Mater.* **2021**, 10, 2002249.
- [67] L. Fan, X. Zhang, M. Nie, Y. Xu, Y. Wang, L. Shang, Y. Zhao, Y. Zhao, *Adv. Funct. Mater.* **2022**, 32, 2110746.
- [68] Y. Hao, Y. Chen, X. He, F. Yang, R. Han, C. Yang, W. Li, Z. Qian, *Bioact. Mater.* **2020**, 5, 542.
- [69] Y. Hao, Y. Chen, M. Lei, T. Zhang, Y. Cao, J. Peng, L. Chen, Z. Qian, *Adv. Ther.* **2018**, 1, 1800008.
- [70] Y. Hao, M. Dong, T. Zhang, J. Peng, Y. Jia, Y. Cao, Z. Qian, *ACS Appl. Mater. Interfaces* **2017**, 9, 15317.
- [71] D. Liu, Y. Zhang, G. Jiang, W. Yu, B. Xu, J. Zhu, *ACS Biomater. Sci. Eng.* **2018**, 4, 1687.
- [72] P. Pei, F. Yang, J. Liu, H. Hu, X. Du, N. Hanagata, S. Zhao, Y. Zhu, *Biomater. Sci.* **2018**, 6, 1414.
- [73] L. Sun, L. Fan, F. Bian, G. Chen, Y. Wang, Y. Zhao, *Research* **2021**, 2021, 9838490.
- [74] Y. Sun, J. Liu, H. Wang, S. Li, X. Pan, B. Xu, H. Yang, Q. Wu, W. Li, X. Su, Z. Huang, X. Guo, H. Liu, *Adv. Funct. Mater.* **2021**, 31, 2100218.
- [75] H. P. Tham, K. Xu, W. Q. Lim, H. Chen, M. Zheng, T. G. S. Thng, S. S. Venkatraman, C. Xu, Y. Zhao, *ACS Nano* **2018**, 12, 11936.
- [76] S. Wei, G. Quan, C. Lu, X. Pan, C. Wu, *Biomater. Sci.* **2020**, 8, 5739.
- [77] T. Wen, Z. Lin, Y. Zhao, Y. Zhou, B. Niu, C. Shi, C. Lu, X. Wen, M. Zhang, G. Quan, *ACS Appl. Mater. Interfaces* **2021**, 13, 48433.
- [78] S. Yao, Y. Wang, J. Chi, Y. Yu, Y. Zhao, Y. Luo, Y. Wang, *Adv. Sci.* **2022**, 9, 2103449.
- [79] Y. Ye, C. Wang, X. Zhang, Q. Hu, Y. Zhang, Q. Liu, D. Wen, J. Milligan, A. Bellotti, L. Huang, G. Dotti, Z. Gu, *Sci. Immunol.* **2017**, 2, eaan5692.
- [80] X. Zhang, G. Chen, Y. Liu, L. Sun, L. Sun, Y. Zhao, *ACS Nano* **2020**, 14, 5901.
- [81] Y. Zhang, G. Jiang, W. Hong, M. Gao, B. Xu, J. Zhu, G. Song, T. Liu, *ACS Appl. Bio Mater.* **2018**, 1, 1906.
- [82] Y. Zhang, D. Wang, M. Gao, B. Xu, J. Zhu, W. Yu, D. Liu, G. Jiang, *ACS Biomater. Sci. Eng.* **2018**, 4, 2879.
- [83] X. Zhou, B. Li, M. Guo, W. Peng, D. Wang, Q. Guo, S. Wang, D. Ming, B. Zheng, *Chem. Eng. J.* **2022**, 427, 131555.
- [84] M. Karimi, P. Sahandi Zangabad, S. Baghaee-Ravari, M. Ghazadeh, H. Mirshekari, M. R. Hamblin, *J. Am. Chem. Soc.* **2017**, 139, 4584.
- [85] D. P. Bhattarai, A. P. Tiwari, B. Maharjan, B. Tumurbaatar, C. H. Park, C. S. Kim, *J. Colloid Interface Sci.* **2019**, 534, 447.
- [86] B. P. Timko, T. Dvir, D. S. Kohane, *Adv. Mater.* **2010**, 22, 4925.
- [87] Y. Yang, L. Xu, D. Jiang, B. Z. Chen, R. Luo, Z. Liu, X. Qu, C. Wang, Y. Shan, Y. Cui, H. Zheng, Z. Wang, Z. L. Wang, X. D. Guo, Z. Li, *Adv. Funct. Mater.* **2021**, 31, 2104092.
- [88] Y. Yang, B. Z. Chen, X. P. Zhang, H. Zheng, Z. Li, C. Y. Zhang, X. D. Guo, *ACS Appl. Mater. Interfaces* **2022**, 14, 31645.
- [89] J. Huang, N. Yap, M. Walter, A. Green, C. Smith, J. Johnson, R. Saigal, *ACS Biomater. Sci. Eng.* **2022**, 8, 1544.
- [90] S. Indermun, Y. E. Choonara, P. Kumar, L. C. Du Toit, G. Modi, S. Van Vuuren, R. Luttge, V. Pillay, *Int. J. Pharm.* **2015**, 496, 351.
- [91] R. Z. Seeni, M. Zheng, D. C. S. Lio, C. Wiraja, M. F. B. Mohd Yusoff, W. T. Y. Koh, Y. Liu, B. T. Goh, C. Xu, *Adv. Funct. Mater.* **2021**, 31, 2105686.
- [92] Y. Wang, X. Zhang, G. Chen, M. Lu, Y. Zhao, *Matter* **2023**, 6, 1555.
- [93] S.-J. Yang, J.-O. Jeong, Y.-M. Lim, J.-S. Park, *Mater. Des.* **2021**, 201, 109485.
- [94] Y.-C. Yang, Y.-T. Lin, J. Yu, H.-T. Chang, T.-Y. Lu, T.-Y. Huang, A. Preet, Y.-J. Hsu, L. Wang, T.-E. Lin, *ACS Appl. Nano Mater.* **2021**, 4, 7917.
- [95] T. Wang, X. Zhang, Z. Wang, X. Zhu, J. Liu, X. Min, T. Cao, X. Fan, *Polymers* **2019**, 11, 1564.
- [96] Z. Deng, T. Hu, Q. Lei, J. He, P. X. Ma, B. Guo, *ACS Appl. Mater. Interfaces* **2019**, 11, 6796.
- [97] S. Indermun, Y. E. Choonara, P. Kumar, L. C. Du Toit, G. Modi, R. Luttge, V. Pillay, *Int. J. Pharm.* **2014**, 462, 52.
- [98] X. Li, X. Huang, J. Mo, H. Wang, Q. Huang, C. Yang, T. Zhang, H.-J. Chen, T. Hang, F. Liu, L. Jiang, Q. Wu, H. Li, N. Hu, Xi Xie, *Adv. Sci.* **2021**, 8, 2100827.
- [99] M. Bok, Y. Lee, D. Park, S. Shin, Z.-J. Zhao, B. Hwang, S. H. Hwang, S. H. Jeon, J.-Y. Jung, S. H. Park, J. Nah, E. Lim, J.-H. Jeong, *Nanoscale* **2018**, 10, 13502.
- [100] S. Xie, J. Huang, A. T. Pereira, L. Xu, D. Luo, Z. Li, *BMEMat* **2023**, 1, e12038.
- [101] K. Ariga, T. Mori, J. P. Hill, *Adv. Mater.* **2012**, 24, 158.
- [102] Y. Zhang, J. Yu, H. N. Bomba, Y. Zhu, Z. Gu, *Chem. Rev.* **2016**, 116, 12536.
- [103] D. Zhang, B. Ren, Y. Zhang, L. Xu, Q. Huang, Y. He, X. Li, J. Wu, J. Yang, Q. Chen, Y. Chang, J. Zheng, *J. Mater. Chem. B* **2020**, 8, 3171.
- [104] J. Di, S. Yao, Y. Ye, Z. Cui, J. Yu, T. K. Ghosh, Y. Zhu, Z. Gu, *ACS Nano* **2015**, 9, 9407.
- [105] J. Yang, Z. Chen, R. Ye, J. Li, Y. Lin, J. Gao, L. Ren, B. Liu, L. Jiang, *Drug Delivery* **2018**, 25, 1728.
- [106] Z. Sun, Y. Hou, *BMEMat* **2023**, 1, e12012.
- [107] V. R. Jayaneththi, K. Aw, M. Sharma, J. Wen, D. Svirskis, A. J. Mcdaid, *Sens. Actuators, B* **2019**, 297, 126708.

- [108] X. Zhang, G. Chen, X. Fu, Y. Wang, Y. Zhao, *Adv. Mater.* **2021**, *33*, 2104932.
- [109] J.-H. Fang, C.-H. Liu, R.-S. Hsu, Y.-Y. Chen, W.-H. Chiang, H.-M. D. Wang, S.-H. Hu, *Polymers* **2020**, *12*, 1392.
- [110] J. Thévenot, H. Oliveira, O. Sandre, S. Lecommandoux, *Chem. Soc. Rev.* **2013**, *42*, 7099.
- [111] Z. Li, Y. Zhou, T. Li, J. Zhang, H. Tian, *View* **2022**, *3*, 20200112.
- [112] H. Lee, T. K. Choi, Y. B. Lee, H. R. Cho, R. Ghaffari, L. Wang, H. J. Choi, T. D. Chung, N. Lu, T. Hyeon, S. H. Choi, D.-H. Kim, *Nat. Nanotechnol.* **2016**, *11*, 566.
- [113] M. Yin, L. Xiao, Q. Liu, S.-Y. Kwon, Y. Zhang, P. R. Sharma, L. Jin, X. Li, B. Xu, *Adv. Healthcare Mater.* **2019**, *8*, 1901170.
- [114] X. Yu, L. Zhu, X. Liang, B. Yuan, M. Li, S. Hu, P. Ding, L. Du, J. Guo, Y. Jin, *Acta Biomater.* **2022**, *146*, 197.
- [115] Y. Zhang, D. Chai, M. Gao, B. Xu, G. Jiang, *Int. J. Polym. Mater. Polym. Biomater.* **2018**, *68*, 850.
- [116] X. Xu, S. Shen, R. Mo, *View* **2022**, *3*, 20200136.
- [117] F. Giusti, A. Martella, L. Bertoni, S. Seidenari, *Pediat. Dermatol.* **2001**, *18*, 93.
- [118] C.-J. Ke, Y.-J. Lin, Y.-C. Hu, W.-L. Chiang, K.-J. Chen, W.-C. Yang, H.-L. Liu, C.-C. Fu, H.-W. Sung, *Biomaterials* **2012**, *33*, 5156.
- [119] A. Ullah, H. Khan, H. J. Choi, G. M. Kim, *Polymers* **2019**, *11*, 1834.
- [120] M. Sardesai, P. Shende, *Curr. Drug Delivery* **2020**, *17*, 776.
- [121] N. W. Kim, M. S. Lee, K. R. Kim, J. E. Lee, K. Lee, J. S. Park, Y. Matsumoto, D.-G. Jo, H. Lee, D. S. Lee, J. H. Jeong, *J. Control Release* **2014**, *179*, 11.
- [122] K. Van Der Maaden, E. Sekerdag, P. Schipper, G. Kersten, W. Jiskoot, J. Bouwstra, *Langmuir* **2015**, *31*, 8654.
- [123] C. Wang, Y. Ye, G. M. Hochu, H. Sadeghifar, Z. Gu, *Nano Lett.* **2016**, *16*, 2334.
- [124] Y. Zhang, Q. Liu, J. Yu, S. Yu, J. Wang, L. Qiang, Z. Gu, *ACS Nano* **2017**, *11*, 9223.
- [125] Q. Jing, H. Ruan, J. Li, Z. Wang, L. Pei, H. Hu, Z. He, T. Wu, S. Ruan, T. Guo, Y. Wang, N. Feng, Y. Zhang, *Biomaterials* **2021**, *278*, 121142.
- [126] H. T. T. Duong, N. W. Kim, T. Thambi, V. H. Giang Phan, M. S. Lee, Y. Yin, J. H. Jeong, D. S. Lee, *J. Control Release* **2018**, *269*, 225.
- [127] H. T. T. Duong, Y. Yin, T. Thambi, T. L. Nguyen, V. H. Giang Phan, M. S. Lee, J. E. Lee, J. Kim, J. H. Jeong, D. S. Lee, *Biomaterials* **2018**, *185*, 13.
- [128] X. Li, Q. Xu, P. Zhang, X. Zhao, Y. Wang, *J. Control Release* **2019**, *314*, 72.
- [129] X. Lan, J. She, D.-A. Lin, Y. Xu, X. Li, W.-F. Yang, V. W. Y. Lui, L. Jin, X. Xie, Y.-X. Su, *ACS Appl. Mater. Interfaces* **2018**, *10*, 33060.
- [130] X. Lan, W. Zhu, X. Huang, Y. Yu, H. Xiao, L. Jin, J. J. Pu, X. Xie, J. She, V. W. Y. Lui, H.-J. Chen, Y.-X. Su, *Nanoscale* **2020**, *12*, 18885.
- [131] Y. Lin, W. Hu, X. Bai, Y. Ju, C. Cao, S. Zou, Z. Tong, C. Cen, G. Jiang, X. Kong, *ACS Appl. Bio Mater.* **2020**, *3*, 6376.
- [132] A. Anderson, C. Hegarty, C. Casimero, J. Davis, *ACS Appl. Mater. Interfaces* **2019**, *11*, 35540.
- [133] J. Zhang, D. Wu, M.-F. Li, J. Feng, *ACS Appl. Mater. Interfaces* **2015**, *7*, 26666.
- [134] B. Xu, Q. Cao, Y. Zhang, W. Yu, J. Zhu, D. Liu, G. Jiang, *ACS Biomater. Sci. Eng.* **2018**, *4*, 2473.
- [135] X.-X. Yang, P. Feng, J. Cao, W. Liu, Y. Tang, *ACS Appl. Mater. Interfaces* **2020**, *12*, 13613.
- [136] H. Sun, P. Saeedi, S. Karuranga, M. Pinkepank, K. Ogurtsova, B. B. Duncan, C. Stein, A. Basit, J. C. N. Chan, J. C. Mbanya, M. E. Pavkov, A. Ramachandran, S. H. Wild, S. James, W. H. Herman, P. Zhang, C. Bommer, S. Kuo, E. J. Boyko, D. J. Magliano, *Diabetes Res. Clin. Prac.* **2022**, *183*, 109119.
- [137] A. N. Naykov, J. P. Mayer, R. D. Dimarchi, *Nat. Rev. Drug Discovery* **2016**, *15*, 425.
- [138] L. A. Donnelly, A. D. Morris, B. M. Frier, J. D. Ellis, P. T. Donnan, R. Durrant, M. M. Band, G. Reekie, G. P. Leese, *Diabetic Med.* **2005**, *22*, 749.
- [139] Y. Ohkubo, H. Kishikawa, E. Araki, T. Miyata, S. Isami, S. Motoyoshi, Y. Kojima, N. Furuyoshi, M. Shichiri, *Diabetes Res. Clin. Prac.* **1995**, *28*, 103.
- [140] G. Chen, J. Yu, Z. Gu, *J. Diabetes Sci. Technol.* **2019**, *13*, 41.
- [141] Q. Wu, Li Wang, H. Yu, J. Wang, Z. Chen, *Chem. Rev.* **2011**, *111*, 7855.
- [142] O. Veis, B. C. Tang, K. A. Whitehead, D. G. Anderson, R. Langer, *Nat. Rev. Drug Discovery* **2015**, *14*, 45.
- [143] J. Yu, Y. Zhang, Y. Ye, R. Disanto, W. Sun, D. Ranson, F. S. Ligler, J. B. Buse, Z. Gu, *Proc. Natl. Acad. Sci. USA* **2015**, *112*, 8260.
- [144] J. Yu, J. Wang, Y. Zhang, G. Chen, W. Mao, Y. Ye, A. R. Kahkoska, J. B. Buse, R. Langer, Z. Gu, *Nat. Biomed. Eng.* **2020**, *4*, 499.
- [145] D. Shen, H. Yu, L. Wang, X. Chen, J. Feng, Q. Zhang, W. Xiong, J. Pan, Y. Han, X. Liu, *J. Mater. Chem. B* **2021**, *9*, 6017.
- [146] C. Yang, T. Sheng, W. Hou, J. Zhang, Li Cheng, H. Wang, W. Liu, S. Wang, X. Yu, Y. Zhang, J. Yu, Z. Gu, *Sci. Adv.* **2022**, *8*, eadd3197.
- [147] Z. Wang, R. Fu, X. Han, D. Wen, Y. Wu, S. Li, Z. Gu, *Adv. Sci.* **2022**, *9*, 2203274.
- [148] M. Wu, Y. Zhang, He Huang, J. Li, H. Liu, Z. Guo, L. Xue, S. Liu, Y. Lei, *Mater. Sci. Eng., C* **2020**, *117*, 111299.
- [149] Z. Guo, H. Liu, Z. Shi, L. Lin, Y. Li, M. Wang, G. Pan, Y. Lei, L. Xue, *J. Mater. Chem. B* **2022**, *10*, 3501.
- [150] Y. Fu, P. Liu, M. Chen, T. Jin, H. Wu, M. Hei, C. Wang, Y. Xu, X. Qian, W. Zhu, *J. Colloid Interface Sci.* **2022**, *605*, 582.
- [151] S. Chen, H. Matsumoto, Y. Moro-Oka, M. Tanaka, Y. Miyahara, T. Suganami, A. Matsumoto, *ACS Biomater. Sci. Eng.* **2019**, *5*, 5781.
- [152] S. Chen, H. Matsumoto, Y. Moro-Oka, M. Tanaka, Y. Miyahara, T. Suganami, A. Matsumoto, *Adv. Funct. Mater.* **2019**, *29*, 1807369.
- [153] S. Chen, T. Miyazaki, M. Itoh, H. Matsumoto, Y. Moro-Oka, M. Tanaka, Y. Miyahara, T. Suganami, A. Matsumoto, *Gels* **2022**, *8*, 74.
- [154] A. Ghavaminejad, J. Li, B. Lu, L. Zhou, L. Lam, A. Giacca, X. Y. Wu, *Adv. Mater.* **2019**, *31*, 1901051.
- [155] B. Lu, A. Ghavaminejad, J. F. Liu, J. Li, S. Mirzaie, A. Giacca, X. Y. Wu, *ACS Appl. Mater. Interfaces* **2022**, *14*, 20576.
- [156] Z. Wang, J. Wang, H. Li, J. Yu, G. Chen, A. R. Kahkoska, V. Wu, Y. Zeng, D. Wen, J. R. Miedema, J. B. Buse, Z. Gu, *Proc. Natl. Acad. Sci. USA* **2020**, *117*, 29512.
- [157] Y. Zhang, M. Wu, D. Tan, Q. Liu, R. Xia, M. Chen, Y. Liu, L. Xue, Y. Lei, *J. Mater. Chem. B* **2021**, *9*, 648.
- [158] R. Mo, T. Jiang, J. Di, W. Tai, Z. Gu, *Chem. Soc. Rev.* **2014**, *43*, 3595.
- [159] D. M. Nathan, P. A. Cleary, J.-Y. C. Backlund, S. M. Genuth, J. M. Lachin, T. J. Orchard, P. Raskin, B. Zinman, *N. Engl. J. Med.* **2005**, *353*, 2643.
- [160] J. Yu, Y. Zhang, W. Sun, A. R. Kahkoska, J. Wang, J. B. Buse, Z. Gu, *Small* **2017**, *13*, 1603028.
- [161] P. Wang, Q. Gong, J. Hu, X. Li, X. Zhang, *J. Med. Chem.* **2020**, *64*, 298.
- [162] R. Li, Z. Jia, M. A. Trush, *React. Oxygen Species* **2016**, *1*, 9.
- [163] J. Liu, M. Wu, R. Zhang, Z. P. Xu, *View* **2021**, *2*, 20200139.
- [164] G. Pizzino, N. Irrera, M. Cucinotta, G. Pallio, F. Mannino, V. Arcoraci, F. Squadrito, D. Altavilla, A. Bitto, *Oxid. Med. Cell. Longevity* **2017**, *2017*, 8416763.
- [165] R. L. Auten, J. M. Davis, *Pediat. Res.* **2009**, *66*, 121.
- [166] F. Gao, Z. Xiong, *Front. Chem.* **2021**, *9*, 649048.
- [167] J. Liang, B. Liu, *Bioeng. Transl. Med.* **2016**, *1*, 239.
- [168] W. Tao, Z. He, *Asia J. Pharma. Sci.* **2018**, *13*, 101.
- [169] X. Hu, J. Yu, C. Qian, Y. Lu, A. R. Kahkoska, Z. Xie, X. Jing, J. B. Buse, Z. Gu, *ACS Nano* **2017**, *11*, 613.
- [170] Z. Tong, J. Zhou, J. Zhong, Q. Tang, Z. Lei, H. Luo, P. Ma, X. Liu, *ACS Appl. Mater. Interfaces* **2018**, *10*, 20014.
- [171] B. Xu, G. Jiang, W. Yu, D. Liu, Y. Zhang, J. Zhou, S. Sun, Y. Liu, *J. Mater. Chem. B* **2017**, *5*, 8200.

- [172] Y. Zhang, J. Wang, J. Yu, D. Wen, A. R. Kahkoska, Y. Lu, X. Zhang, J. B. Buse, Z. Gu, *Small* **2018**, *14*, 1704181.
- [173] C. Song, X. Zhang, M. Lu, Y. Zhao, *Research* **2023**, *6*, 0119.
- [174] Y. Zhou, L. Yang, Y. Lyu, D. Wu, Y. Zhu, J. Li, D. Jiang, X. Xin, L. Yin, *Int. J. Nanomed.* **2023**, *18*, 899.
- [175] M. S. Shim, Y. Xia, *Angew. Chem.* **2013**, *125*, 7064.
- [176] F. Liu, Z. Cheng, H. Yi, J. *Nanobiotechnol.* **2023**, *21*, 1.
- [177] A. Raza, U. Hayat, T. Rasheed, M. Bilal, H. M. N. Iqbal, *Eur. J. Med. Chem.* **2018**, *157*, 705.
- [178] H. Qu, J. Yang, S. Li, Ji Xu, X. Zhou, X. Xue, D. Zhang, H. Du, Y. Shen, M. Ramachandran, H. Zheng, Y. Wu, Y. Ding, H. Wu, X. Ma, T.-Y. Lin, Y. Li, *J. Control Release* **2023**, *357*, 274.
- [179] R. De La Rica, D. Aili, M. M. Stevens, *Adv. Drug Delivery Rev.* **2012**, *64*, 967.
- [180] Q. Hu, P. S. Katti, Z. Gu, *Nanoscale* **2014**, *6*, 12273.
- [181] M.-R. Lee, K.-H. Baek, H. J. Jin, Y.-G. Jung, I. Shin, *Angew. Chem.-Int. Ed.* **2004**, *43*, 1675.
- [182] Y. Ye, J. Wang, Q. Hu, G. M. Hochu, H. Xin, C. Wang, Z. Gu, *ACS Nano* **2016**, *10*, 8956.
- [183] Y. Zhang, J. Yu, J. Wang, N. J. Hanne, Z. Cui, C. Qian, C. Wang, H. Xin, J. H. Cole, C. M. Gallippi, Y. Zhu, Z. Gu, *Adv. Mater.* **2017**, *29*, 1604043.
- [184] M. Mir, A. D. Permana, N. Ahmed, G. M. Khan, A. U. Rehman, R. F. Donnelly, *Eur. J. Pharm. Biopharm.* **2020**, *147*, 57.
- [185] M. Mir, A. D. Permana, I. A. Tekko, H. O. McCarthy, N. Ahmed, A. U. Rehman, R. F. Donnelly, *Int. J. Pharm.* **2020**, *587*, 119643.
- [186] A. D. Permana, Q. K. Anjani, Sartini, E. Utomo, F. Volpe-Zanutto, A. J. Paredes, Y. M. Evary, S. A. Mardikasari, M. R Pratama, I. N. Tuany, R. F. Donnelly, *Mater. Sci. Eng., C* **2021**, *120*, 111786.
- [187] W. Hu, Z. Wang, Y. Zha, X. Gu, W. You, Y. Xiao, X. Wang, S. Zhang, J. Wang, *Adv. Healthcare Mater.* **2020**, *9*, 2000035.
- [188] T. R. Dargaville, B. L. Farrugia, J. A. Broadbent, S. Pace, Z. Upton, N. H. Voelcker, *Biosens. Bioelectron.* **2013**, *41*, 30.
- [189] Q. Pang, D. Lou, S. Li, G. Wang, B. Qiao, S. Dong, L. Ma, C. Gao, Z. Wu, *Adv. Sci.* **2020**, *7*, 1902673.
- [190] M. Guo, Y. Wang, B. Gao, B. He, *ACS Nano* **2021**, *15*, 15316.
- [191] Y. Wang, H. Lu, M. Guo, J. Chu, B. Gao, B. He, *Adv. Healthcare Mater.* **2022**, *11*, 2101659.
- [192] J. Chi, X. Zhang, C. Chen, C. Shao, Y. Zhao, Y. Wang, *Bioact. Mater.* **2020**, *5*, 253.
- [193] J. Li, M. Zeng, H. Shan, C. Tong, *Curr. Med. Chem.* **2017**, *24*, 2413.
- [194] S. Ruan, Y. Zhang, N. Feng, *Biomater. Sci.* **2021**, *9*, 8065.
- [195] H. Sung, J. Ferlay, R. L. Siegel, M. Laversanne, I. Soerjomataram, A. Jemal, F. Bray, *Ca-Cancer J. Clin.* **2021**, *71*, 209.
- [196] F. Bray, M. Laversanne, E. Weiderpass, I. Soerjomataram, *Cancer* **2021**, *127*, 3029.
- [197] W. Guo, Z. Chen, L. Tan, D. Gu, X. Ren, C. Fu, Q. Wu, X. Meng, *View* **2022**, *3*, 20200174.
- [198] Y. Lee, T. Kang, H. R. Cho, G. J. Lee, O. K. Park, S. Kim, B. Lee, H. M. Kim, G. D. Cha, Y. Shin, W. Lee, M. Kim, H. Kim, Y. M. Song, S. H. Choi, T. Hyeon, D.-H. Kim, *Adv. Mater.* **2021**, *33*, 2100425.
- [199] Y. Ding, Y. Wang, Q. Hu, *Exploration* **2022**, *2*, 20210106.
- [200] G. Stingl, G. Steiner, *Curr. Problems Dermatol.* **1989**, *18*, 22.
- [201] H. Monaco, S. Yokomizo, H. S. Choi, S. Kashiwagi, *View* **2022**, *3*, 20200110.
- [202] J. Lin, S. Wang, P. Huang, Z. Wang, S. Chen, G. Niu, W. Li, J. He, D. Cui, G. Lu, X. Chen, Z. Nie, *ACS Nano* **2013**, *7*, 5320.
- [203] R. Allison, K. Moghissi, G. Downie, K. Dixon, *Photodiagn. Photodyn. Ther.* **2011**, *8*, 231.
- [204] E. Hussein, M. Zagho, G. Nasrallah, A. Elzatahy, *Int. J. Nanomed.* **2018**, *13*, 2897.
- [205] Y. Li, G. He, L.-H. Fu, M. R. Younis, T. He, Y. Chen, J. Lin, Z. Li, P. Huang, *ACS Nano* **2022**, *16*, 17298.
- [206] C. Wang, Y. Zeng, K.-F. Chen, J. Lin, Q. Yuan, X. Jiang, G. Wu, F. Wang, Y.-G. Jia, W. Li, *Bioact. Mater.* **2023**, *27*, 58.
- [207] Y. Sun, M. Chen, D. Yang, W. Qin, G. Quan, C. Wu, X. Pan, *Nano Res.* **2022**, *15*, 2335.
- [208] C. Iglesias-Lopez, A. Agustí, M. Obach, A. Vallano, *Front. Pharmacol.* **2019**, *10*, 921.
- [209] D.-W. Zheng, Q. Lei, J.-Y. Zhu, J.-X. Fan, C.-X. Li, C. Li, Z. Xu, S.-X. Cheng, X.-Z. Zhang, *Nano Lett.* **2017**, *17*, 284.
- [210] T. Wang, G. Chen, S. Zhang, D. Li, G. Wei, X. Zhao, Y. Liu, D. Ding, X. Zhang, *Nano Lett.* **2023**, *23*, 7990.
- [211] S. J. Welsh, P. G. Corrie, *Ther. Adv. Med. Oncol.* **2015**, *7*, 122.
- [212] P. B. Chapman, A. Hauschild, C. Robert, J. B. Haanen, P. Ascierto, J. Larkin, R. Dummer, C. Garbe, A. Testori, M. Maio, D. Hogg, P. Lorigan, C. Lebbe, T. Jouary, D. Schadendorf, A. Ribas, S. J. O'day, J. A. Sosman, J. M. Kirkwood, A. M. M. Eggermont, B. Dreno, K. Nolop, J. Li, B. Nelson, J. Hou, R. J. Lee, K. T. Flaherty, G. A. Mcarthur, *N. Engl. J. Med.* **2011**, *364*, 2507.
- [213] A. Ribas, K. T. Flaherty, *Nat. Rev. Clin. Oncol.* **2011**, *8*, 426.
- [214] X. Cheng, S. Hu, K. Cheng, *ACS Nano* **2023**, *17*, 11855.
- [215] J. Zhao, W. Duan, X. Liu, F. Xi, J. Wu, *Adv. Funct. Mater.* **2023**, *33*, 2308183.



Huaqing Chu received her Bachelor's degree from Shanxi Medical University in 2018. She is currently an M.D. student at the Department of Anesthesiology, National Cancer Center/Cancer Hospital, Chinese Academy of Medical Sciences, and Peking Union Medical College. Her research interests mainly focus on drug-loaded microneedles and wearable electronics.



Jiangtao Xue received his Bachelor's degree from Beijing Institute of Technology in 2016. He is currently a Ph.D. student at the School of Medical Technology, Beijing Institute of Technology. His research interests mainly focus on nanogenerators and wearable electronics.



Yuan Yang received her Ph.D. from the University of Chinese Academy of Sciences in 2022, and her master's degree from the Beijing University of Chemical Technology in 2019. Currently, she is a post-doctor at the Institute of Process Engineering, Chinese Academy of Sciences. Her research interests include microneedles, drug delivery, and biomaterials.



Hui Zheng received his M.D. and Ph.D. from Beijing Tuberculosis Chest Tumor Institute in 2008, and a Bachelor's Degree from Harbin Medical University in 1992. He worked as a visiting scholar at Massachusetts General Hospital, Harvard Medical School in 2011. He currently is a professor, chief physician, and doctoral tutor at the Department of Anesthesiology, National Cancer Center/Cancer Hospital, Chinese Academy of Medical Sciences, and Peking Union Medical College. His research focuses on basic research of neurodevelopment and neurotoxicity and anesthesia-related clinical translational research.



Dan Luo received his B.Sc. and Ph.D. degrees at Peking University Health Science Center in 2008 and 2013, respectively. He worked at the Institute of Chemistry, Chinese Academy of Sciences in 2013, then transferred to China University of Petroleum-Beijing in 2015. Since 2021, he has joined the Beijing Institute of Nanoenergy and Nanosystems, Chinese Academy of Sciences as a professor. His research focuses on physiotherapy strategies based on self-powered devices.



Zhou Li received his Ph.D. from Peking University in the Department of Biomedical Engineering in 2010, and his Bachelor's Degree from Wuhan University in 2004. He joined the School of Biological Science and Medical Engineering of Beihang University in 2010 as an Associate Professor. Currently, he is a Professor at the Beijing Institute of Nanoenergy and Nanosystems, Chinese Academy of Sciences. His research interests include nanogenerators, in vivo energy harvesters, self-powered medical devices, and biosensors.